การประมาณน้ำหนักของรถบรรทุกขณะเคลื่อนที่จากค่าความเร่งสะพาน

นางสาวบาร์บาร่า แอกนีสกา ซูชิโอ

วิทยานิพนธ์นี้เป็นส่วนหนึ่งของการศึกษาตามหลักสูตรปริญญาวิศวกรรมศาสตรมหาบัณฑิต
สาขาวิชาวิศวกรรมโยธา ภาควิชาวิศวกรรมโยธา
คณะวิศวกรรมศาสตร์ จุฬาลงกรณ์มหาวิทยาลัย
ปีการศึกษา 2558

WEIGHT ESTIMATION OF MOVING TRUCK FROM BRIDGE ACCELERATIONS

Miss Barbara Agnieszka Szucio

A Thesis Submitted in Partial Fulfillment of the Requirements

for the Degree of Master of Engineering Program in Civil Engineering

Department of Civil Engineering

Faculty of Engineering

Chulalongkorn University

Academic Year 2015

Thesis Title	WEIGHT ESTIMATION OF MOVING TRUCK FROM BRIDGE ACCELERATIONS
By	Miss Barbara Agnieszka Szucio
Field of Study	Civil Engineering
Thesis Advisor	Associate ProfessorTospol Pinkaew, Ph.D.

Accepted by the Faculty of Engineering, Chulalongkorn University in Partial Fulfillment of the Requirements for the Master's Degree

.....Dean of the Faculty of Engineering

(ProfessorSupot Teachavorasinskun, Ph.D.)

THESIS COMMITTEE

.....Chairman

(ProfessorTeerapong Senjuntichai, Ph.D.)

.....Thesis Advisor

(Associate ProfessorTospol Pinkaew, Ph.D.)

.....External Examiner

(Associate ProfessorNakhorn Poovarodom, Ph.D.)

บาร์บาร่า แอกนีสกา ซูชิโอ : การประมาณน้ำหนักของรถบรรทุกขณะเคลื่อนที่จากค่าความเร่งสะพาน (WEIGHT ESTIMATION OF MOVING TRUCK FROM BRIDGE ACCELERATIONS) อ.ที่ปรึกษาวิทยานิพนธ์หลัก: รศ. ดร.ทศพล ปิ่นแก้ว, 73 หน้า.

น้ำหนักรถในโครงข่ายจราจรเป็นข้อมูลสำคัญในการออกแบบและวางแผนบำรุงรักษาถนนและสะพาน แม้มีหลายวิธีที่จะใช้หาน้ำหนักรถบรรทุก วิธีการใช้สะพานชั่งน้ำหนัก (B-WIM) ได้รับความนิยมมากขึ้นเนื่องจากผู้ขับรถไม่สามารถมองเห็นและระบบสามารถเคลื่อนย้ายได้ อย่างไรก็ดีระบบ B-WIM นี้มักใช้สัญญาณจากหัววัดความเครียดที่ติดตั้งใต้สะพานมาประมาณน้ำหนักรถ การวิจัยนี้จึงศึกษาความเห็นไปได้และประสิทธิภาพของระบบ B-WIM ที่ใช้สัญญาณความเร่งของสะพานแทน เพราะหัววัดความเร่งติดตั้งได้ง่ายกว่าและมีราคาถูกกว่า สำหรับวิธีการหาน้ำหนักรถได้นำวิธีการ average acceleration discrete algorithm ซึ่งใช้หาค่าแรงกระทำต่ออาคารได้ดีมาพัฒนาและปรับใช้กับกรณีที่แรงกระทำต่อสะพานจากรถมีการเคลื่อนที่ ในการศึกษาได้จำลองปฏิสัมพันธ์ของรถและสะพานด้วยสมการคณิตศาสตร์ แล้วนำค่าความเร่งของสะพานที่ได้ไปใช้ประมาณค่าน้ำหนักรถที่แล่นผ่านสะพาน โดยกระบวนการ inverse identification เพื่อให้ค่าคาดการณ์ความเร่งใกล้เคียงกับค่าความเร่งที่เกิดขึ้นมากที่สุด งานวิจัยนี้พิจารณาสะพานแบบช่วงเดียวมีรถบรรทุกเคลื่อนที่ผ่าน ผลการหาค่าน้ำหนักบรรทุกถูกนำไปเปรียบเทียบกับค่าน้ำหนักจริงกรณีที่รถมีระยะห่างเพลา น้ำหนักบรรทุก และความเร็วต่างๆ สุดท้ายจึงอภิปรายถึงความเป็นไปได้และประสิทธิภาพในการใช้ค่าความเร่งแทนค่าความเครียดในการประมาณน้ำหนักของรถบรรทุกขณะเคลื่อนที่ข้ามสะพาน

ภาควิชา วิศวกรรมโยธา ลายมือชื่อนิสิต .....

สาขาวิชา วิศวกรรมโยธา ลายมือชื่อ อ.ที่ปรึกษาหลัก .....

ปีการศึกษา 2558

5770520521 : MAJOR CIVIL ENGINEERING

KEYWORDS: WEIGHT ESTIMATION / LOAD IDENTIFICATION / MOVING LOAD / ACCELERATION RESPONSE

BARBARA AGNIESZKA SZUCIO: WEIGHT ESTIMATION OF MOVING TRUCK FROM BRIDGE ACCELERATIONS. ADVISOR: ASSOC. PROF.TOSPOL PINKAEW, Ph.D., 73 pp.

Vehicular weight in road network is crucial information for road and bridge design and maintenance. Many methods of weight identification have been proposed. The bridge weigh-in-motion (B-WIM) method is an alternative that becomes more popular due to its difficult visibility by the truck drivers and portability. Existing bridge weigh-in-motion (B-WIM) system utilizes the signals from strain gauges installed beneath the bridges to estimate the weight of the moving vehicles. Therefore, this research studies the feasibility and effectiveness of weight determination of moving vehicles from bridge accelerations since the installation of accelerometers is more convenient and much cheaper. The average acceleration discrete algorithm which was found to be effective to identify the non-moving dynamic loads acting on buildings is selected and extended to the case of moving load identification of truck passing over the bridge. To study the effectiveness of the proposed weight estimation method, the vehicle-bridge interaction is simulated. The obtained bridge acceleration is employed as the input for weight estimation of passing truck. This load estimation is an inverse identification problem. Numerical examples of a simply-supported bridge under passing truck are conducted to investigate the accuracy and efficiency of the proposed method. Effects of the axle spacing, mass and speed of vehicle on the accuracy of the identification results are reported.

Department:	Civil Engineering	Student's Signature	.....
Field of Study:	Civil Engineering	Advisor's Signature	.....
Academic Year:	2015		

ACKNOWLEDGEMENTS

CONTENTS

Page

Page

1. Introduction

1.1 Background and Research Motivation

Vehicular weight on a bridge deck is crucial information for bridge design and maintenance. Bridge design is mainly dominated by heavy trucks, which produce large impact loading and can cause serious structural damages. Even though the weight limit regulations are specified, the truck overloading is becoming an increasing problem. To enforce the weight limit requirements in the transportation network, weight stations have been installed. Traditionally, the vehicle is measured directly, which is both time consuming and expensive due to the price of weigh pad. The required stop of all heavy truck on the highway can cause queuing and induce traffic congestion. A wide range of alternative methods of indirect weight identification have been proposed in the last few years. The most important objectives of these methods are to detect the vehicle weights without disturbing the traffic flow and to decrease the cost of this process.

The first proposed methods are based on the estimating the vehicle axle weights using strain response or bending moments of the bridge. The researches proved that these methods provided high accuracy and efficiency and they were robust for force identification in engineering practices. However due to the fact that the price of strain gauges is high and they are difficult to install, the other type of bridge response was proposed to be used in force identification.

The newest idea of force identification in the vehicle-bridge system is based on dynamic response. Recently some research investigations have been conducted to provide the method of force identification using acceleration response. The new method explored by Ding et al. (2013) has attracted my attention. The research explores the average acceleration discrete algorithm, which is very promising in the future application. However the accuracy of the proposed algorithm relies only on the numerical simulation and the simple experimental investigation. That is why there is a need for continued research and application of this idea.

The objective of this dissertation is to extend the Ding's algorithm. The force identification technique is modified for different type of loading. The problem of moving vehicle over the bridge is studied. The purpose is to calculate the weight of the moving vehicle with high accuracy and the low cost of future application. Main advantage of proposed method is that it requires only finite element model of the structure and accelerometers. The axle sensors should be placed at the entry and exit of the bridge deck to obtain required information about vehicle such as moving speed and axle spacing. The numerical study on computer simulation will be provided to validate the effectiveness of a proposed method.

1.2 Objectives

- To numerically model the vehicle-bridge interaction.
- To apply the average acceleration method to identify the dynamic axle loads and weight of moving vehicle from bridge deck acceleration.
- To evaluate the performance and effectiveness of the adopted method.

1.3 Scope

- 2D linear bridges simplified as simply supported uniform beam.
- Single truck with two axles moving over the bridge deck with constant velocity.

1.4 Methodology

The purpose of this study is to estimate vehicular weight on a bridge deck. The force identification method is proposed to estimate weight of a moving truck based on the Ding's research (2013). The average acceleration method which was found to be effective to identify the dynamic loads on buildings is selected and extended to the case of moving load identification of truck passing over a bridge. The algorithm for weight

estimation of moving vehicle is derived. The bridge acceleration is used as the input data in the calculation. Computer simulation is conducted using MATLAB software in order to validate the proposed method and investigate the effectiveness of weight estimation. The proposed scheme of this study is presented in a flowchart.

In this study, the vehicle-bridge interaction is numerically simulated to obtain acceleration response. The Newmark-β method is proposed to solve coupled equation. The obtained bridge acceleration is employed as the input for weight estimation of passing truck.To address the accuracy of derived force identification method, four numerical examples are investigated.

The study begins with the simplest system in which the bridge is modeled as single-degree-of-freedom system (SDOF). The second numerical system is Multi Degree of Freedom System with a non-moving load placed at the mid-span. The bridge structure is modelled as single span simply supported beam and is discretized by finite element method using beam elements. These two examples are studied to check the influence of different time varying amplitude load functions on accuracy of dynamic force identification. The third system is a moving point load over the bridge deck. In all above cases, the accuracy of identified dynamic loads is investigated. The percentage error is defined as the norm of difference between the real and the identified force to the norm of the real one. Additionally, to address the accuracy of identified forces, reproduction of responses from identified dynamic force is made using Newmark-β method. The reproduced responses of the bridge, such as acceleration, velocity and displacement are compared with the real ones.

REVIEWED ARTICLES

- Vehicle-bridge interaction
- Strain or displacement based identification
- Acceleration based identification

THEORY - DERIVATION

- Vehicle-bridge interaction
- Average acceleration algorithm to identify axle dynamic loads of moving vehicle over the bridge (Ding et al., 2013)

NUMERICAL STUDY

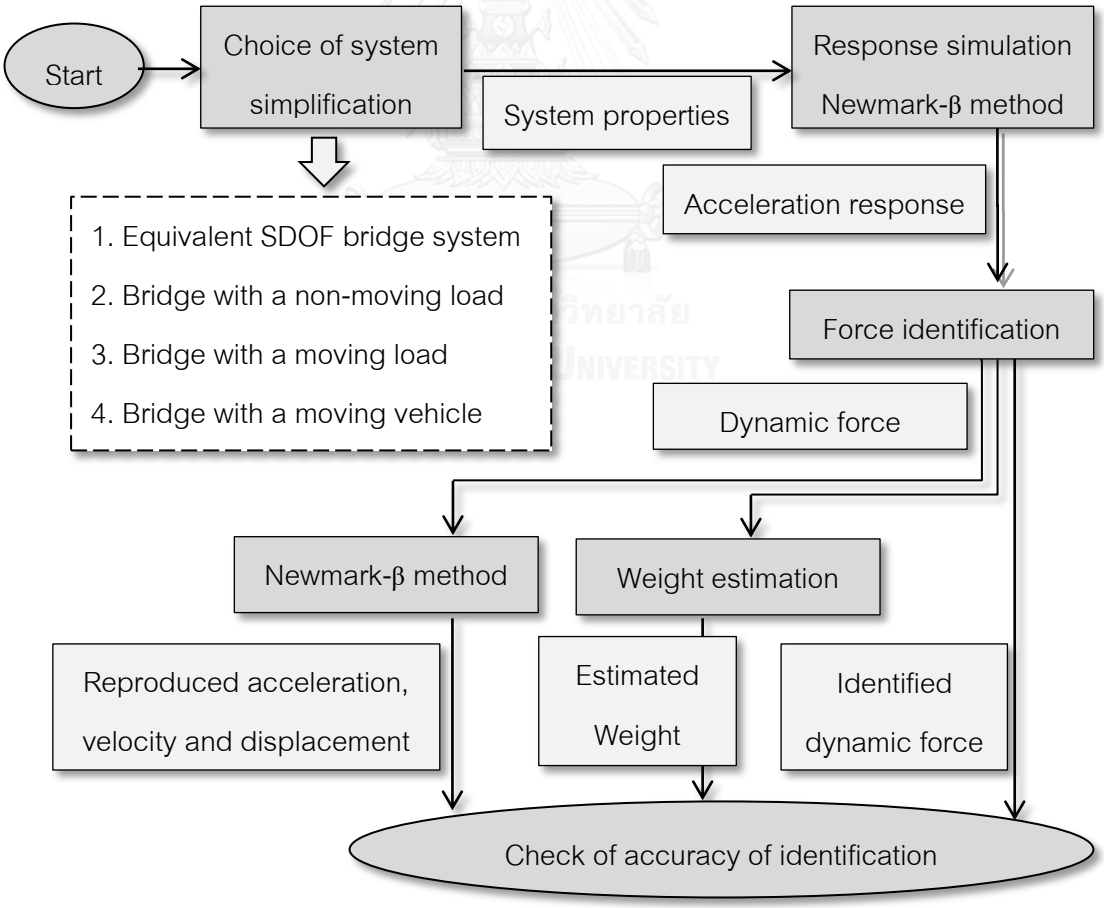

DISCUSSION OF ACCURACY

The last numerical system is a moving vehicle over the bridge. The vehicle is simplified as a dynamic model with 4 degrees of freedom moving over the bridge deck with the constant speed. The moving load is assumed to be always in contact with the bridge surface throughout the duration of travel. The last numerical example addresses not only accuracy of identified dynamic force but also weight estimation of the truck. Three accelerometers are assumed to be installed beneath the bridge and are employed in identification. The errors of dynamic load of front axle, rear axle and summation of axles are calculated. The system of two dynamic forces moving over the bridge is solved to reproduce the responses.

When the accuracy of identification of dynamic axle loads is addressed, the idea of weight estimation is defined. The weight of each axle is assumed to be the average of dynamic force. Time duration, in which the identification of dynamic force is the most accurate, is taken as representative for the weight estimation of axles. Percentage errors between real and identified axle weight are calculated. All simulations are conducted with varying of parameters of passing truck such as speed, weight and axle spacing to study accuracy and limits of the proposed method for future application.

The discussion and the suggestion for actual application are provided at the end of the study based on the effectiveness of dynamic force identification and truck weight estimation.

2. Literature review

2.1 General

The discussion will include a review of the relevant literature in order to provide a broader understanding of vehicle-bridge interaction and different methods for force identification used throughout the last few years.

2.2Vehicle-bridge interaction

The major objective of WIM system is to identify the axle loads of vehicle. That is why a large body of research has been published on vehicle-bridge interaction to investigate identification methods.

Fryba (1973) studied vibration of solids and structures under moving loads. The first chapter is focused on one-dimensional solids subjected to loads that vary in both time and space called moving loads. The book broadens knowledge about the dynamic effects of different speed and weights of vehicle on the simply supported beam.

Henchi et al. (1998) proposed an efficient algorithm for dynamic analysis of bridges under moving vehicles. A bridge is discretized by a three-dimensional finite element model with dynamic system of vehicles running at a prescribed speed. Vehicle is modeled as a linear discrete mass-spring-damper system. The two ways to simulate the dynamic interaction are given. The first way is to solve the uncoupled iteration method, in which bridge and vehicles systems are solved separately and then an iterative process in each time step is performed to find the equilibrium between the bridge and vehicle tires. The second idea is to simulate the dynamic interaction between bridge and vehicle. The paper presented a way to find a solution of this coupled system based on modal superposition method for the bridge structure and the physical components for the vehicles using Lagrange's formulation.

Green and Cebon (1997) explored the dynamic interaction between heavy vehicles and highway bridges. The iterative method is presented for calculating the dynamic

response of bridges to dynamic wheel loads. A simply supported bridge is subjected to a single degree of freedom vehicle model(lumped mass supported by spring and damper).The method is validated by field tests on a highway bridge and concludes whether the bridge-vehicle interaction is important or can be ignored and treated as uncoupled.

Yang (1999) derived a versatile element for analyzing vehicle–bridge interaction (VBI) response, in which Newmark finite difference scheme was used to discretize the vehicle equations of motion. Through use of the no-jump condition for vehicles, the contact forces can be related to the contact displacements of the bridge. The proposed method is versatile because it allows us to deal with vehicle models of various complexities. The paper focused on the problem of train-bridge interaction due to its complexity. The effect of the suspension system of the vehicles should be considered if the riding comfort is a concern. The other major problem of analyzing VBI response is an unknown number of vehicles, which leads to the great range of sophisticated models used in simulations. The first step in analyzing the vehicle–bridge interaction systems is to write two equations of motion of the second order for the vehicles and the bridge. Then the two subsystems are coupled based on the interaction forces existing at the contact points. The matrices are time-dependent, therefore they have to be updated and factorized at each time step in an incremental analysis.

The paper described different approaches to find a solution. The one way is to use iteration method in which the vehicle equation is solved to obtain the interaction forces and then proceed to solve the bridge equations for improved values of displacements for the contact points. The poor convergence rate is the main drawback of this method while solving a problem with a large number of vehicles. The other way to solve the VBI problems is based on the condensation method. Some condensation methods relate the vehicle (slave) DOFs to the bridge (master) DOFs. However these methods are efficient only for computing the bridge response, not for computing the vehicle response. Instead of accurate master–slave relations, the Newmark finite difference scheme has been

established in this research to discretize the vehicle equation, which contributes good results and is suitable for handling both the vehicle and bridge responses.

Yang and Lin (2005) studied “Vehicle–bridge interaction dynamics and potential applications”. Based on the method of modal superposition, closed-form solutions are obtained for the vertical responses of both the bridge and moving vehicle, assuming the vehicle-bridge mass ratio to be small. Method considering only first mode gives quite good accuracy. The different types of vehicle models are explained such as moving load, moving mass and sprung mass models. The paper studied a simply supported beam subjected to a moving sprung mass. Two sets of second order differential equations of motion have to be written. Thanks to contact force existing between the two subsystems, the two sets of equations become nonlinear and coupled. The proposed method was validated by field tests and compared with the results from another method. The accuracy of this analytical method is better than the accuracy of solution obtained based on finite element analysis.

2.3 Vehicle Force identification

2.3.1 Strain or displacement based identification

The conventional WIM (Weigh-in-motion) systems have been explored in a considerable amount of researches for many years. The accuracy of estimation of static load from the measurements of dynamic impact forces has been improved greatly through new approaches and more sophisticated numerical models. The robustness of a wide range of algorithms of force prediction has been proved by both numerical simulations and field tests.

Law et al. (1997) explored the time-domain identification method for axle loads on the bridge. The paper contained the analytical solution derivation and the test. Bridge is modeled as a simply supported beam. The modal superposition principle is used in the method. The procedure is shown for both a single force identification and two moving forces identification. Both the simulations and laboratory experiments show that data

from bending moment and acceleration measurements can be used to obtain axle forces accurately and effectively. However, the large error occurs at the time when axles approach and leave the bridge.

Chan et al. (1999) proposed a closed-form solution method for moving force identification. The method is an inverse study in which the Euler beam associated with modal analysis is used to identify moving loads from bridge responses. The paper contained also recommended number of strain gauges.

Chan et al. (2000) theoretically and experimentally conducted the comparative studies on moving force identification from bridge strains. A theoretical study of force identification using prestressed concrete bridges was conducted. Moving forces across a prestressing bridge are identified from strain gauge measurements. The accuracy of those identified forces is significantly affected by noise. The method is applied to a field test on an existing prestressed concrete bridge in Hong Kong. In other paper, the comparative studies on moving force identification were conducted in laboratory. The moving forces were identified from the bridge strains using the four methods. It was proved that the Time-domain method (TDM) had the best accuracy and was highly recommended.

What is more, Chan et al. (2000) also studied moving force identification using an existing prestressed concrete bridge. The field measurements were conducted of a two-axle heavy vehicle over real bridge. The forces are identified based on the above time-domain method. Clearly, this shows that the method is robust for force identification in engineering practices.

European Commission DG VII – Transport: WAVE (2001) developed another identification technique for moving loads on bridge using least-square method with optimization technique. Since the axle loads are assumed to be constants on the bridge, the parameters in the optimization become velocity, number of axles, axle spacing and total weight. Two-dimensional bridge model is used to study the effect of eccentricity of the bridge. The field test was investigated to verify the accuracy of identification. The results show that the static load of vehicle has error in the range of ±10 %.

Zhu and Law (2002) proposed a new method to identify moving loads on the bridge taking into account road surface roughness and incomplete vehicle speed. Validation of the given method is proved by not only numerical studies a single and multiple-span bridges but also the experiment using only strain gauges. Furthermore in numerical studies, the force identification conducted from accelerations gives better results than from strains. The acceleration is less sensitive to the noise level however a bigger number of modes is required. The proposed method with the assumption of average speed is also accurate with the vehicle which is braking on the bridge.

Yu and Chan (2004) applied the frequency–time domain method to identify the multi-axle vehicle loads from the measured bending moment response. The method was tested in laboratory by fabricated bridge–vehicle system model.

Law et al. (2004) proposed vehicle axle loads identification method based on finite element method and condensation technique using strain measurements. The measured displacements are expressed as the shape functions without the modal coordinate transformation. Numerical simulations and experimental results show the efficiency and accuracy of the method to identify moving loads.

Zhu and Law (2005) developed a moving load identification algorithm for multi-span continuous bridge with elastic supports. In the paper the effects of the wide variety of parameters are studied such as the measuring noise, sampling rate, vertical and rotational stiffness. The method based on modal superposition and regularization technique is adopted. The vertical translation and rotational springs are included in the model to simulate the elastic bearings and support fixity conditions of the bridge. It is shown that identified forces are more accurate when measured acceleration is used in calculation. For high frequency of the excitation forces the greater number of vibration modes is required to obtain an accurate solution. The paper proved that the proposed method can be used to solve problems with elastic restraints.

Pinkaew (2006) established updated static component technique for identification of vehicle axle loads. The main objective of the new method is to calculate the vehicle weight from the bridge strain responses without any disturbance due to the vehicle's

traveling speed. Instead of the least-squares method, the updated static component (USC) technique is proposed, which is not sensitive to an assigned regularization parameter. The numerical examples of a two-axle vehicle moving on a simply-supported bridge subjected to different speeds of the vehicle and surface roughness amplitudes of the bridge are conducted. The experiments proved the accuracy of the proposed method.

Wu and Law (2010) developed moving force identification based on stochastic finite element model. A statistical relationship between the random moving force and the random structural responses is established to formulate a general stochastic force identification algorithm. Numerical simulations prove effectiveness of the algorithm.

More recently Xun Xu and Jinping Ou (2015) proposed the method for “Force identification of dynamic systems using virtual work principle”. This research indicated a moving least square (MLS) method, which is one of the load reconstructed methods for identifying the dynamic force. The method contained three main parts.

The first part was responsible for obtaining the expressions of the unknown acting force at each moment. However before identification it is crucial to face some difficulties such as the number of loads and the unknown individual values in time history. Method is simplified by reducing the number of unknowns by defining force as a series of known primary functions with unknown coefficients. In the research, Chebyshev orthogonal basis functions are used as primary functions to express impact force and structural responses. This approach reduces the calculating time and gives high accuracy. The main idea of force identification is to change the differential equation to integral equation based on the virtual work principle. Thanks to this, the method eliminates errors which are connected with calculating the structural acceleration and velocity response. What is more, there is no need to integrate and make iteration process to get a fitting solution. Additionally the method is general for all types of forces due to the fact that shape functions are always the same with different coefficients.

The second part is focused on solving the equation of motion. Due to the fact that direct solving the differential equations is very difficult, the other method is proposed.

The Fourier transform and the inverse frequency response function (IFSF) method are used to transform the governing equation into the product of the frequency response function and external load. These two techniques have also some drawbacks, for instance, numerical instability for the resonance frequency or other errors due to very short load duration. The previous studies proposed to use modal orthogonality to simplify a problem however it may cause truncation errors and the instability for the ill-conditioned matrix. Avoiding the calculation of the matrix inversion is also the advantage.

The last part is focused on assuring the stability of the solution and dealing with random noises. Using numerical methods, it is crucial to be aware of the error of measured data, the error of discretization and round-off error. In this paper, the two methods are proposed to deal with ill-conditioned problems, such as Tikhonov regularization method and truncated singular value decomposition (TSVD).

The validation of proposed method is proved by three examples. The first two are numerical simulations of a four-degree-of-freedom dynamic system and a cantilever beam. The results are compared with actual applied force to calculate the relative error. The noise impact is controlled by the signal-to-noise ratio (SNR). The significant influence on the accuracy has not only noise level but also the pace of disturbances. It is proved that harmonic force is better identified and more immunes to noise than arbitrary force. The last example is an experimental model of a cantilever beam, which checked the application of this method with different structures. Due to a certain error between the real structure and the FEA model, the model was improved by the structural frequency measured. The results are slightly less accurate than from previous examples because of difficulty of correct noise's identification and the FEA model error.

2.3.2 Acceleration based identification

The alternative idea of force identification is to use accelerometers instead of strain gauges. The major advantage of application of accelerometers is that their installation is much easier and they are more practically attractive.

Xu et al. (2010) explored stress and acceleration analysis of coupled vehicle (train) and long-span bridge systems. The mode superposition method is presented analyzing only the resonance condition. The Tsing Ma Bridge in Hong Kong was selected as a case study. It was proved that proposed method could be used to predict stressed without installing strain gauges.

Lu and Liu (2011) described a method to identify both damages in bridge deck and vehicular parameters using acceleration measurements. This approach is based on dynamic response sensitivity-based finite element model. Through examples, it is shown that the proposed method has potential for real application of damage detection and parameter identification.

More recent studies, Ding et al. (2013) investigated the "Average acceleration discrete algorithm for force identification in state space" and revealed quite good results. The validation of the proposed method is checked on three structures.

Firstly, a three-dimensional three-storey frame is numerically investigated with single and multiple random excitations. The investigation of the method's accuracy includes measurement noise, model error and unexpected environmental disturbances.

Secondly, a seven-storey planar frame is tested in a laboratory. The frame on the bottom is connected firmly to the ground and two lumped mass are placed on each floor. The stiffness of the structure is calculated by the optimization function 'fmincon'. The impact force is the horizontal hammer impact applied at the peak.

Finally, a scaled model of a fourteen-storey concrete shear wall building with additional steel frame is subjected to shaking table simulating seismic excitation. A scale ratio is 1/6; the steel frame is constructed with the rubber isolation. This experiment enables to study the horizontal interaction between the steel frame and the shear wall building.

The investigation of the method's accuracy includes measurement noise, model error and unexpected environmental disturbances. Without any noise and model error the method is very accurate. Adding different percentage number of measurement noise, model error or unexpected random base excitation show that force identification

can be still fairly accurate. The study also explores two other existing force identification algorithms to provide the check of the results. These discrete algorithms are the First-Order-Hold (FOH) and the Zeroth-Order-Hold (ZOH).

The results both from numerical simulations and from laboratory tests prove that the proposed method can be successfully used to identify external excitations by the structural acceleration responses. Another advantage is that the method needs only finite element model of the structure and accelerometers. It is important to recognize that the idea of force identification with average acceleration discrete algorithm is used only for structures subjected to seismic excitations in numerical simulations and simple laboratory tests. The method has not been tested for real structures or different types of an impact force yet.

Qiao et al. (2015) proposed a force identification method based on wavelet multi-resolution analysis using cubic B-spline scaling functions. Instead of solving the original governing equation of force identification, the coefficients of scaling functions, which yield a well-posed problem, have to be found. Force identification laboratory experiments are conducted on a cantilever beam to check the accuracy of the proposed method. The cantilever beam structure is applied for impact and harmonic force identification. The measured data is the acceleration response. Results are compared with the results based on the truncated singular value decomposition (TSVD) technique.

Wang et al. (2015) presented a novel state space method for force identification based on the Galerkin weak formulation using the discretization idea of the Finite Element Method and the refined version for the case of high noise level. The method is more suitable for the cases of large time step and discontinuous loading compared with the conventional state space method and the explicit Newmark method. Numerical studies are conducted to evaluate the performance of the GW method on plane truss structure. In the experiments the measured acceleration responses are used in force identification. The method is proved to be conditionally stable and second-order accurate.

Feng et al. (2015) studied simultaneous identification of bridge structural parameters and vehicle loads. The previous methods are based on a model with known system parameters, therefore this research proposed a method which can be used not only to identify vehicle dynamic axle loads but also to identify bridge structural parameters such as flexural stiffness and damping ratio or the road roughness. This possibility is beneficial, because the dynamic effects can be rapidly increased by road roughness.

Firstly, dynamics of the VBI system are defined such as road surface roughness, vehicle model and bridge model. The Newmark-β method is proposed to solve the vehicle-bridge coupled equation. Secondly, an iterative procedure is developed to address the inverse problem for simultaneous identification of bridge structural parameters and vehicle axle loads from a limited number of response measurements. Then, a Bayesian inference-based regularization technique is used to solve the ill-posed problem of force identification. The measurement data is bridge acceleration response. The objective of an iterative parametric optimization process is to minimize the error between the measured and predicted system responses. Herein, the algorithm of this iterative procedure is given. Numerical analyses of a simply-supported single-span bridge and a three-span continuous bridge are conducted to investigate the accuracy and efficiency of the proposed method. The errors occur only at the instances when the moving vehicle enters and exits the bridge. The accuracy of solution can be improved by increasing the number of sensors.

To sum, although previous research investigations provide some insight into force identification from acceleration response there is a need for continued research and application of this idea. Further investigation should be conducted in order to modify this method for different types of problem.

All recent methods are interesting however they have not been proved sufficiently yet. For instance, Qiao et al. (2015) proved their method only by simple laboratory experiments conducted on a cantilever beam. Wang et al. (2015) conducted only numerical studies on plane truss structure. Feng et al. (2015) showed numerical

analyses of a bridge with moving load. In contrast to the above researches, the Ding et al. (2013) method is proved not only by numerical simulations but also by laboratory tests. The paper contains a numerical investigation of three-dimensional three-storey frame, a laboratory test of a seven-storey planar frame and a scaled model of a fourteen-storey concrete shear wall building subjected to shaking table simulating seismic excitation.

Although previous researches have been numerically and experimentally studied and have shown that the external loads can be accurately predicted from acceleration responses. They have overlooked a fundamental issue where it is impossible to predict using only acceleration data such as static load case. Therefore this study will focus firstly on the fundamental of load prediction from acceleration response by considering some simple load patterns to understand the identification behavior. Then a more realistic vehicle-bridge system is investigated. The identification technique is extended form Ding (2013) and Feng (2015).

3. Theory

3.1 General

Since it is difficult to measure the moving forces directly, this chapter is focused on techniques to measure indirectly the vehicle loads from measured acceleration response of the bridge. Firstly vehicle-bridge interaction is presented. In order to simulate the vehicle bridge-interaction, coupled system of bridge and vehicle is solved at each time step. Secondly the concept of axle load identification is derived using measured acceleration response.

3.2 Vehicle-bridge interaction

The vehicle-bridge interaction model is described based on the finite element method. This concept has been studied by Deesomsuk (2008).

3.2.1 Vehicle Model

The vehicle model is present in Figure 3.1. The vehicle moving at a speed *v(t)* over a bridge. There are 4 degrees of freedom in the vehicle model consisting of vertical displacement, rotation of vehicle mass, vertical displacement of front and rear axle suspension mass. The equation of motion can be derived by dynamic equilibrium of the vehicle system in each degree of freedom as shown in Figure 3.2.

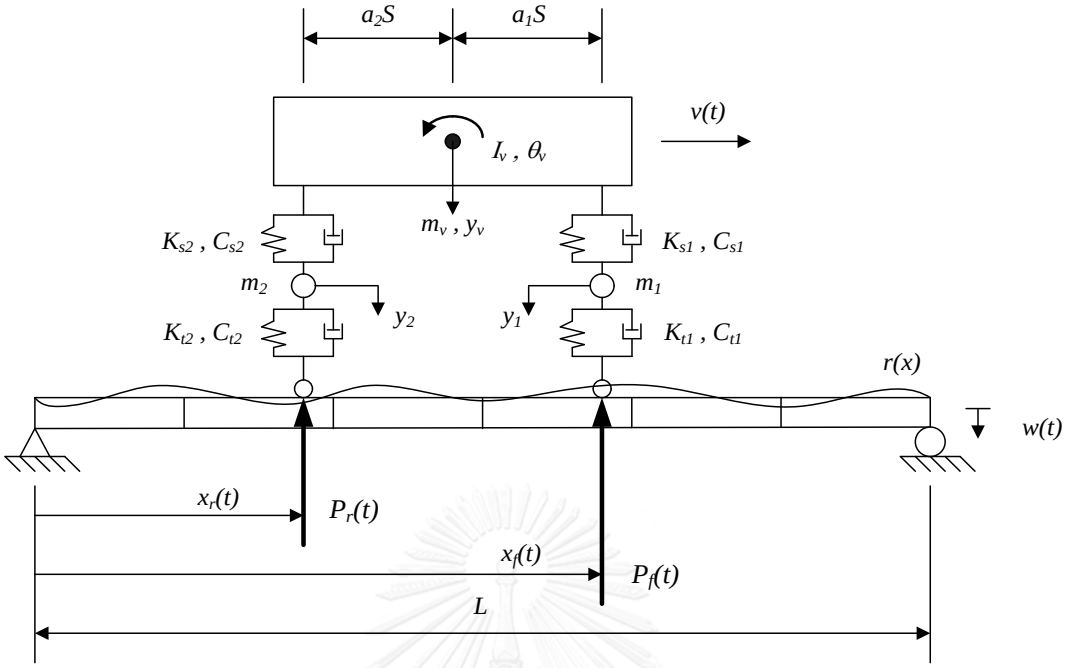

Figure 3.1 Vehicle-bridge system

Let m_v – mass of the vehicle

I_v – mass rotational moment of inertia of the vehicle

m_1 – mass of front axle suspension

m_2 – mass of rear axle suspension

K_{s1}, K_{s2} – suspension stiffness of front and rear axle

C_{s1}, C_{s2} – suspension damping of front and rear axle

K_{t1}, K_{t2} – tire stiffness of front and rear axle

C_{t1}, C_{t2} – tire damping of front and rear axle

S – axle spacing

L – span length of bridge

$x_f(t), x_r(t)$ – positions of the front and rear axle respectively at time t

$P_f(t), P_r(t)$ – front and rear axle force respectively at time t

v – velocity of vehicle

θ_v – rotation of vehicle mass

y_v – vertical displacement of vehicle

y_1, y_2 – vertical displacement of front and rear suspension mass

$w(t)$ – vertical dynamic deflection of bridge

a_1, a_2 – center of gravity ratio of vehicle from front and rear axle.

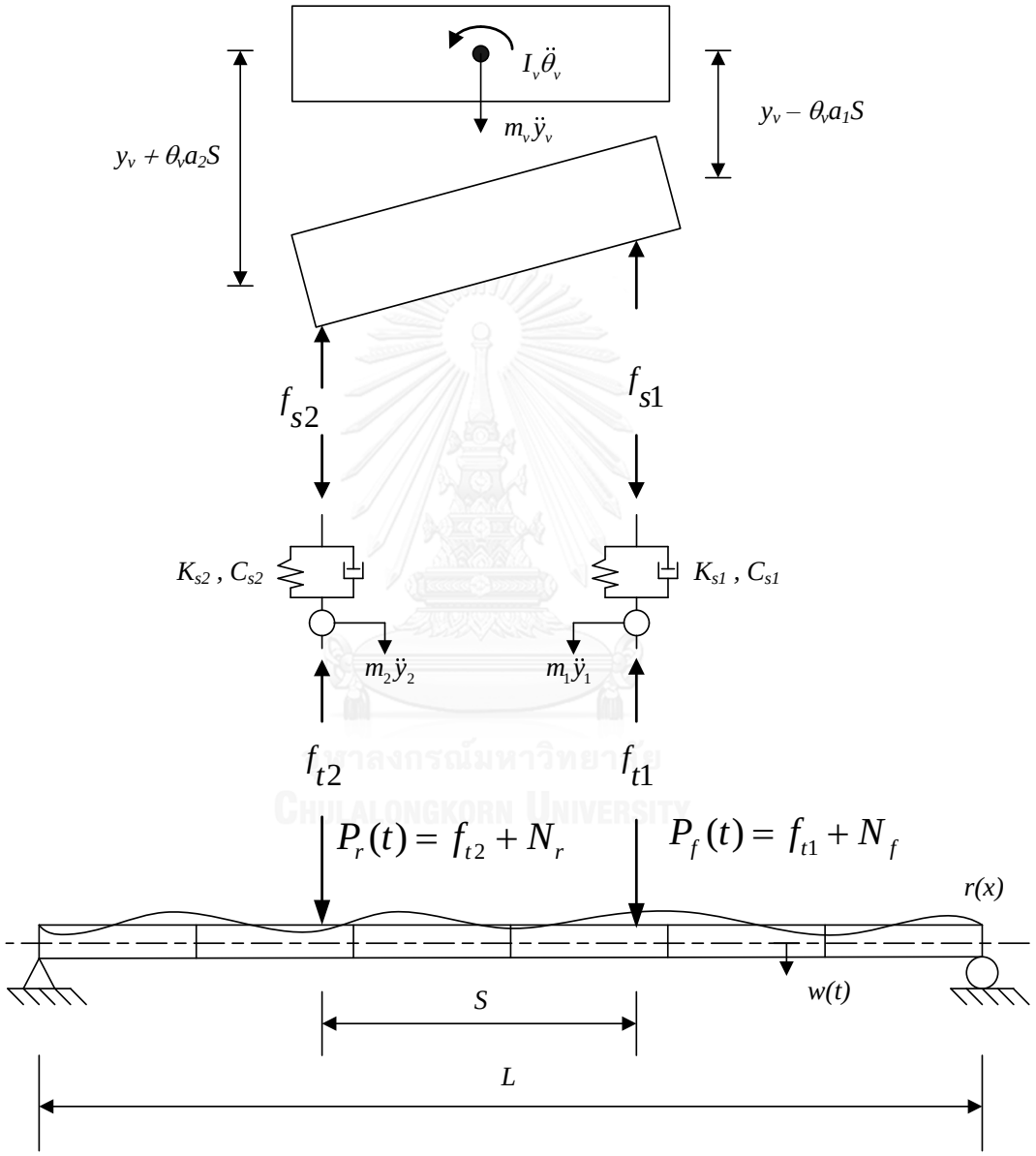

Figure 3.2 Free body diagram of vehicle-bridge system

The vertical force equilibrium of vehicle mass:

$$\sum F = m_v\ddot{y}_v \quad ; \qquad -f_{s1} - f_{s2} = m_v\ddot{y}_v \tag{3.1}$$

where

$$f_{s1} = K_{s1}(y_v - \theta_v a_1 S - y_1) + C_{s1}(\dot{y}_v - \dot{\theta}_v a_1 S - \dot{y}_1)$$
$$f_{s2} = K_{s2}(y_v + \theta_v a_2 S - y_2) + C_{s2}(\dot{y}_v + \dot{\theta}_v a_2 S - \dot{y}_2).$$

Using above equations, equilibrium of vehicle mass of vertical motion becomes:

$$m_v\ddot{y}_v + (C_{s1} + C_{s2})\dot{y}_v + (K_{s1} + K_{s2})y_v$$
$$+(-C_{s1}a_1 S + C_{s2}a_2 S)\dot{\theta}_v + (-K_{s1}a_1 S + K_{s2}a_2 S)\theta_v \quad (3.2)$$
$$+(-C_{s1})\dot{y}_1 + (-K_{s1})y_1 + (-C_{s2})\dot{y}_2 + (-K_{s2})y_2 = 0$$

Consider rotation of vehicle mass at center of gravity:

$$\sum M_c = I_v\ddot{\theta}_v \quad ; \qquad f_{s1}a_1 S - f_{s2}a_2 S = I_v\ddot{\theta}_v \quad (3.3)$$

Replacing f_{s1}, f_{s2} in (3.3), equilibrium of rotation of vehicle mass will become:

$$I_v\ddot{\theta}_v + (-C_{s1}a_1 S + C_{s2}a_2 S)\dot{y}_v + (-K_{s1}a_1 S + K_{s2}a_2 S)y_v$$
$$+(C_{s1}a_1^2 S^2 + C_{s2}a_2^2 S^2)\dot{\theta}_v + (K_{s1}a_1^2 S^2 + K_{s2}a_2^2 S^2)\theta_v \quad (3.4)$$
$$+(C_{s1}a_1 S)\dot{y}_1 + (K_{s1}a_1 S)y_1 + (-C_{s2}a_2 S)\dot{y}_2 + (-K_{s2}a_2 S)y_2 = 0$$

Consider the vertical equilibrium of suspension massm_1:

$$\sum F = m_1\ddot{y}_1 \quad ; \qquad f_{s1} - f_{t1} = m_1\ddot{y}_1 \quad (3.5)$$

where

$$f_{t1} = K_{t1}(y_1 - \Delta_1) + C_{t1}(\dot{y}_1 - \dot{\Delta}_1)$$
$$\Delta_1 = w_1(x_f(t), t)$$
$$\dot{\Delta}_1 = \dot{w}_1(x_f(t), t)$$

Replacing f_{s1}, f_{t1} in Eq. (3.5), equilibrium of vertical motion of suspension mass m_1 will become:

$$m_1\ddot{y}_1 + (-C_{s1})\dot{y}_v + (-K_{s1})\dot{y}_v + (C_{s1}a_1 S)\dot{\theta}_v + (K_{s1}a_1 S)\theta_v$$
$$+(C_{s1})\dot{y}_1 + (K_{s1})y_1 = -f_{t1} \quad (3.6)$$

The vertical equilibrium of suspension mass m_2:

$$\sum F = m_2\ddot{y}_2 \quad ; \qquad f_{s2} - f_{t2} = m_2\ddot{y}_2 \quad (3.7)$$

where

$$f_{t2} = K_{t2}(y_2 - \Delta_2) + C_{t2}(\dot{y}_2 - \dot{\Delta}_2)$$

$$\Delta_2 = w_2(x_r(t), t)$$

$$\dot{\Delta}_2 = \dot{w}_1(x_r(t), t)$$

Replacing f_{s2}, f_{t2} in Eq. (3.7), equilibrium of vertical motion of suspension mass m_2 is:

$$\begin{aligned} &m_2\ddot{y}_2 + (-C_{s2})\dot{y}_v + (-K_{s2})y_v + (-C_{s2}a_2S)\dot{\theta}_v + (-K_{s2}a_2S)\theta_v \\ &+(C_{s2})\dot{y}_2 + (K_{s2})y_2 = -f_{t2} \end{aligned} \tag{3.8}$$

Thus, the equations of motion for the vehicle are transformed into matrix form using Eq. (3.2), (3.4), (3.6) and (3.08):

$$M_v\ddot{Y}(t) + C_v\dot{Y}(t) + K_vY(t) = P_v(t) \tag{3.9}$$

where

$$M_v = \begin{bmatrix} m_v & 0 & 0 & 0 \\ 0 & I_v & 0 & 0 \\ 0 & 0 & m_1 & 0 \\ 0 & 0 & 0 & m_2 \end{bmatrix}$$

$$C_v = \begin{bmatrix} C_{s1} + C_{s2} & (-C_{s1}a_1 + C_{s2}a_2)S & -C_{s1} & -C_{s2} \\ (-C_{s1}a_1 + C_{s2}a_2)S & (C_{s1}a_1^2 + C_{s2}a_2^2)S & C_{s1}a_1S & -C_{s2}a_2S \\ -C_{s1} & C_{s1}a_1S & C_{s1} & 0 \\ -C_{s2} & -C_{s2}a_2S & 0 & C_{s2} \end{bmatrix}$$

$$K_v = \begin{bmatrix} K_{s1} + K_{s2} & (-K_{s1}a_1 + K_{s2}a_2)S & -K_{s1} & -K_{s2} \\ (-K_{s1}a_1 + K_{s2}a_2)S & (K_{s1}a_1^2 + K_{s2}a_2^2)S & K_{s1}a_1S & -K_{s2}a_2S \\ -K_{s1} & K_{s1}a_1S & K_{s1} & 0 \\ -K_{s2} & -K_{s2}a_2S & 0 & K_{s2} \end{bmatrix}$$

$$Y(t) = \{y_v(t) \quad \theta_v(t) \quad y_1(t) \quad y_2(t)\}^T$$

P_v is the force terms containing the interaction force vector and static force vector as follows:

$$P_v(t) = -\begin{Bmatrix} 0 \\ P_{int}(t) \end{Bmatrix} + \begin{Bmatrix} 0 \\ M_s \end{Bmatrix} = -\begin{Bmatrix} 0 \\ 0 \\ P_f(t) \\ P_r(t) \end{Bmatrix} + \begin{Bmatrix} 0 \\ 0 \\ N_f \\ N_r \end{Bmatrix} \tag{3.10}$$

where

$$P_f(t) = (f_{t1}(t) + N_f) = K_{t1}(y_1(t) - \Delta_1(t)) + C_{t1}(\dot{y}_1(t) - \dot{\Delta}_1(t)) + N_f$$

$$P_r(t) = (f_{t2}(t) + N_r) = K_{t2}(y_2(t) - \Delta_2(t)) + C_{t2}(\dot{y}_2(t) - \dot{\Delta}_2(t)) + N_r$$

$$N_f = (m_1 + a_2 m_v)g$$

$$N_r = (m_2 + a_1 m_v)g$$

3.2.2 Bridge Model

The bridge structure is considered as a simply supported beam and is discretized by finite element method using beam elements as shown in Figure 3.2. The finite beam element has 2 nodes with respect to 4 degrees of freedom in vertical displacement and rotational displacement at both ends as shown in Figure 3.3.

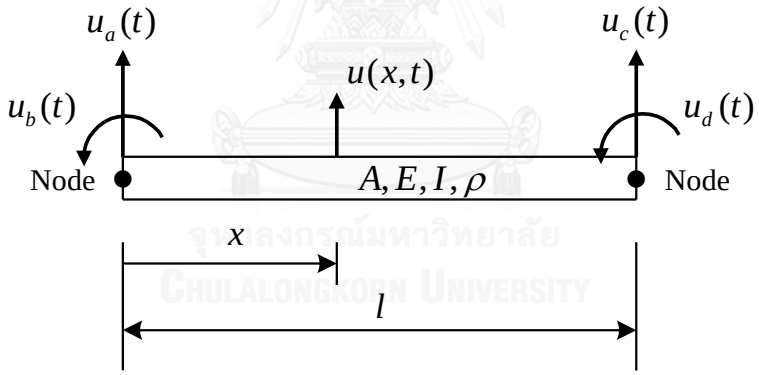

Figure 3.3 Finite beam element with 4 degrees of freedom

where

A – cross section area of beam element

E – modulus of elasticity of beam element

I – moment of inertia of beam element

ρ – mass per unit length of beam element

l – length of beam element.

Let $u(x,t)$ is the deflection of the bridge at distance *x* at time *t*. Thus, the governing equation of beam at position x and at time t can be expressed by:

$$\frac{\partial^2}{\partial x^2}\left[EI\frac{\partial^2 u(x,t)}{\partial x^2}\right] = 0 \tag{3.11}$$

For the bridge having constantEI, Eq. (3.11) can be rewritten as:

$$\frac{\partial^4 u(x,t)}{\partial x^4} = 0 \tag{3.12}$$

The solution of Eq. (3.12) can be expressed in polynomial form as:

$$u(x,t) = c_1(t)x^3 + c_2(t)x^2 + c_3(t)x + c_4(t) \tag{3.13}$$

where $c_i(t)$ is the coefficient of the polynomial form with constant value.

The boundary conditions of beam element are:

$$\begin{aligned} u(0,t) &= u_1(t) & u(l,t) &= u_3(t) \\ \frac{\partial u(0,t)}{\partial x} &= u_2(t) & \frac{\partial u(l,t)}{\partial x} &= u_4(t) \end{aligned} \tag{3.14}$$

Substituting (3.13) in Eq. (3.14), the constant values become:

$$\begin{aligned} c_4(t) &= u_1(t) \\ c_3(t) &= u_2(t) \\ c_2(t) &= \frac{1}{l^2}[3(u_3 - u_1) - l(2u_2 + u_4)] \\ c_1(t) &= \frac{1}{l^3}[2(u_1 - u_3) - l(u_2 + u_4)] \end{aligned} \tag{3.15}$$

Substituting (3.15) in Eq. (3.13), one can write the displacement equation of beam element at position x and at time t as follow:

$$\begin{aligned} u(x,t) = &\left[1 - \frac{3x^2}{l^2} + \frac{2x^3}{l^3}\right]u_1(t) + l\left[\frac{x}{l} - \frac{2x^2}{l^2} + \frac{x^3}{l^3}\right]u_2(t) \\ &+ \left[\frac{3x^2}{l^2} - \frac{2x^3}{l^3}\right]u_3(t) + l\left[-\frac{x^2}{l^2} + \frac{x^3}{l^3}\right]u_4(t) \end{aligned} \tag{3.16}$$

The shape functions of displacements of a beam element are the coefficient terms in front of $u_i(t)$.

The mass matrix of beam element is defined by substituting Eq. (3.16) in equation of kinetic energy:

$$T(t) = \frac{1}{2}\int_0^l \rho A\left[\frac{\partial u(x,t)}{\partial t}\right]^2 dx \tag{3.17}$$

Then, Eq. (3.17) becomes as:

$$T(t) = \frac{1}{2}\dot{u}^T M\dot{u} \tag{3.18}$$

Where the elemental mass matrix is M and the time derivative of the elemental displacement vector $u(t)$ is $\dot{u}$.

$$u(t) = \begin{bmatrix} u_1(t) \\ u_2(t) \\ u_3(t) \\ u_4(t) \end{bmatrix} \tag{3.19}$$

The elemental mass matrix of beam element is obtained by substituting Eq. (3.16) and Eq. (3.19) in Eq. (3.18).

$$M = \frac{\rho Al}{420} \begin{bmatrix} 156 & 22l & 54 & -13l \\ 22l & 4l^2 & 13l & -3l^2 \\ 54 & 13l & 156 & -22l \\ -13l & -3l^2 & -22l & 4l^2 \end{bmatrix} \tag{3.20}$$

As the mass matrix, the stiffness matrix can be calculated by substituting Eq. (3.16) in strain energy equation:

$$V(t) = \frac{1}{2} \int_0^l EI \left[\frac{\partial^2 u(x,t)}{\partial x^2} \right]^2 dx \tag{3.21}$$

The Eq. (3.21) can be written as:

$$V(t) = \frac{1}{2} u^T K u \tag{3.22}$$

Using $u(t)$ which is determined in Eg. (3.19), the stiffness matrix of a beam element can be expressed as:

$$\mathrm{K} = \frac{EI}{l^3} \begin{bmatrix} 12 & 6l & -12 & 6l \\ 6l & 4l^2 & -6l & 2l^2 \\ -12 & -6l & 12 & -6l \\ 6l & 2l^2 & -6l & 4l^2 \end{bmatrix} \tag{3.23}$$

The equation of motion of bridge is:

$$M_b \ddot{R}(t) + C_b \dot{R}(t) + K_b R(t) = P_b(t) \tag{3.24}$$

where M_b – mass matrix of the bridge

C_b – damping matrix of the bridge

K_b – stiffness matrix of the bridge

$R(t)$ – global response vector of the bridge

$P_b(t)$ – external acting load vector of the bridge, which is the interaction force expressed as nodal loads at bridge's degrees of freedom.

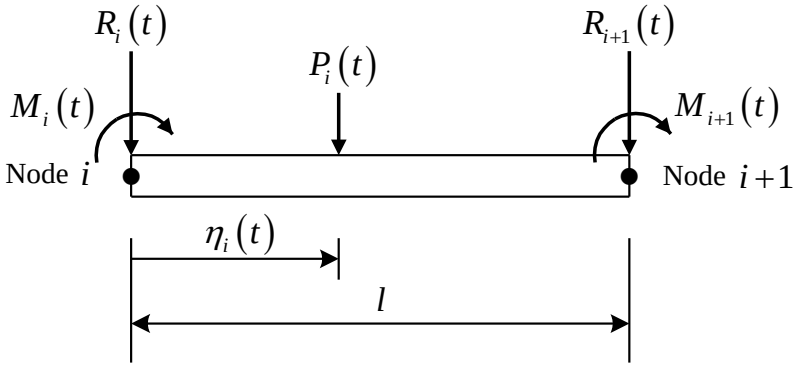

Figure 3.4 Nodal loads from external load

$\eta_i(t)$ – the distance between the left node of element and the external acting load $P_i(t)$.

The nodal loads transformed from external load become:

$$R_i(t) = \left(1 - \frac{3\eta_i(t)^2}{l^2} + \frac{2\eta_i(t)^3}{l^3}\right) P_i(t) \tag{3.25}$$

$$M_i(t) = \left(\eta_i(t) - \frac{2\eta_i(t)^2}{l} + \frac{\eta_i(t)^3}{l^2}\right) P_i(t) \tag{3.26}$$

$$R_{i+1}(t) = \left(\frac{3\eta_i(t)^2}{l^2} - \frac{2\eta_i(t)^3}{l^3}\right) P_i(t) \tag{3.27}$$

$$M_{i+1}(t) = \left(\frac{\eta_i(t)^3}{l^2} - \frac{\eta_i(t)^2}{l}\right) P_i(t) \tag{3.28}$$

where

$R_i(t), R_{i+1}(t)$ – vertical load of node $i^{th}$and $i+1^{th}$

M_i, M_{i+1} – bending moment of node $i^{th}$and $i+1^{th}$.

The shape function of the j^{th} element which is used to calculate the nodal load vector from the external acting load can be expressed as:

$$H_j = \left\{1 - 3\left(\frac{\eta}{l}\right)^2 + 2\left(\frac{\eta}{l}\right)^3 \quad \eta\left(\frac{\eta}{l} - 1\right)^2 \quad 3\left(\frac{\eta}{l}\right)^2 - 2\left(\frac{\eta}{l}\right)^3 \quad \eta\left(\frac{\eta}{l}\right)^2 - \frac{\eta^2}{l}\right\}^T \tag{3.29}$$

For the global external load shape function, the above equation becomes:

$$H_c = \begin{Bmatrix} 0 & \cdots & 0 & \cdots & 0 & \cdots & H_1 & \cdots & 0 \\ 0 & \cdots & 0 & \cdots & H_i & \cdots & 0 & \cdots & 0 \\ 0 & \cdots & H_{N_p} & \cdots & 0 & \cdots & 0 & \cdots & 0 \end{Bmatrix}^T \tag{3.30}$$

where

H_c – an $NN \times N_p$ matrix with zero entries except at the degrees of freedom corresponding to the nodal displacements of the beam elements on which the load is acting,

NN – the number of degrees of freedom of the bridge after considering the boundary condition,

N_p – the number of external acting loads.

Using the relationship between the nodal load and the global load, the interaction force between bridge and vehicle is expressed as:

$$P_b(t) = H_c\big(x(t)\big) \cdot P_{int}(t) \tag{3.31}$$

$$P_{int}(t) = \Big\{P_1(t), P_2(t), \dots, P_{N_p}(t)\Big\}^T \tag{3.32}$$

where

$P_b(t)$ – nodal load vector of bridge

$H_c\big(x(t)\big)$ – transformation vector from external loads to nodal loads

$P_{int}(t)$ – vector of vehicle-bridge interaction force with respect to number of axles.

Then, the equation of motion for bridge becomes:

$$M_b\ddot{R}(t) + C_b\dot{R}(t) + K_bR(t) = H_c\big(x(t)\big)P_{int}(t) \tag{3.33}$$

3.2.3 Vehicle-Bridge Interaction

All degrees of freedom of vehicle and bridge must be solved simultaneously to formulate the vehicle-bridge interaction as the equation of motion of the vehicle-bridge system.

When vehicle with the number of axles $N_p = 2$ is considered, the interaction force vector becomes:

$$\begin{aligned} P_{int}(t) &= \begin{Bmatrix} P_f(t) \\ P_r(t) \end{Bmatrix} \\ &= \begin{Bmatrix} K_{t1}\left(y_1(t) - w_1\big(x_f(t),t\big)\right) + C_{t1}\left(\dot{y}_1(t) - \dot{w}_1\big(x_f(t),t\big)\right) \\ K_{t2}\big(y_2(t) - w_2(x_r(t),t)\big) + C_{t2}\big(\dot{y}_2(t) - \dot{w}_2(x_r(t),t)\big) \end{Bmatrix} \\ &+ \begin{Bmatrix} (m_1 + a_2m_v)g \\ (m_2 + a_1m_v)g \end{Bmatrix} \end{aligned} \tag{3.34}$$

It is observed that the Eq. (3.34) contains vehicle's and bridge's degrees of freedom.

When $R(t)$ is obtained, the deflection of bridge at position x and at time t can be obtained from:

$$w(x,t) = {H_c}^T\big(x(t)\big) \cdot R(t) \tag{3.35}$$

The time derivative of bridge's deflection is

$$\dot{w}(x,t) = \frac{\partial {H_c}^T(x(t))}{\partial x} \cdot R(t) \cdot \dot{x}(t) + {H_c}^T\big(x(t)\big) \cdot \dot{R}(t). \tag{3.36}$$

Substituting Eq. (3.35) and (3.46) in Eq. (3.34) yields

$$\begin{aligned} P_f(t) &= K_{t1}\left(y_1(t) - {H_c}^T\left(x_f(t)\right) \cdot R(t)\right) \\ &+C_{t1}\left(\dot{y}_1(t) - \frac{\partial {H_c}^T\left(x_f(t)\right)}{\partial x} \cdot R(t) \cdot v(t) - {H_c}^T\left(x_f(t)\right) \cdot \dot{R}(t)\right) + (m_1 + a_2 m_v)g \\ P_r(t) &= K_{t2}\left(y_2(t) - {H_c}^T\big(x_r(t)\big) \cdot R(t)\right) \\ &+C_{t2}\left(\dot{y}_2(t) - \frac{\partial {H_c}^T(x_r(t))}{\partial x} \cdot R(t) \cdot v(t) - {H_c}^T\big(x_r(t)\big) \cdot \dot{R}(t)\right) + (m_2 + a_1 m_v)g \end{aligned} \tag{3.37}$$

The Eq. (3.37) can be rewritten in matrix form as:

$$\begin{aligned} \begin{Bmatrix} P_f(t) \\ P_r(t) \end{Bmatrix} &= \begin{bmatrix} K_{t1} & 0 \\ 0 & K_{t2} \end{bmatrix} \cdot \begin{Bmatrix} y_1(t) \\ y_2(t) \end{Bmatrix} + \begin{bmatrix} C_{t1} & 0 \\ 0 & C_{t2} \end{bmatrix} \cdot \begin{Bmatrix} \dot{y}_1(t) \\ \dot{y}_2(t) \end{Bmatrix} \\ &- \begin{bmatrix} K_{t1} \cdot {H_c}^T\left(x_f(t)\right) + C_{t1} \cdot v(t) \cdot \frac{\partial {H_c}^T\left(x_f(t)\right)}{\partial x} \\ K_{t2} \cdot {H_c}^T\big(x_r(t)\big) + C_{t2} \cdot v(t) \cdot \frac{\partial {H_c}^T(x_r(t))}{\partial x} \end{bmatrix} \cdot \{R(t)\} \\ &- \begin{bmatrix} C_{t1} \cdot {H_c}^T\left(x_f(t)\right) \\ C_{t2} \cdot {H_c}^T\big(x_r(t)\big) \end{bmatrix} \cdot \{\dot{R}(t)\} + \begin{Bmatrix} (m_1 + a_2 m_v) \cdot g \\ (m_2 + a_1 m_v) \cdot g \end{Bmatrix} \end{aligned} \tag{3.38}$$

Introducing Eq. (3.38) into the vehicle's equation of motion (3.9), the equilibrium for the vehicle degrees of freedom becomes

$$\begin{aligned} &\left[\begin{array}{c|cc} 0 & 0 & 0 \\ \hline 0 & M_{v1} & 0 \\ 0 & 0 & M_{v2} \end{array}\right]\begin{bmatrix} \ddot{R} \\ \hline \ddot{Y} \end{bmatrix} + \left[\begin{array}{c|cc} 0 & 0 & 0 \\ \hline 0 & C_{v11} & C_{v12} \\ -C_t H_c^T & C_{v21} & C_{v22} \end{array}\right]\begin{bmatrix} \dot{R} \\ \hline \dot{X} \end{bmatrix} \\ &+ \left[\begin{array}{c|cc} 0 & 0 & 0 \\ \hline 0 & K_{v11} & K_{v12} \\ -K_t H_c^T - C_t v \frac{\partial H_c^T}{\partial x} & K_{v21} & K_{v22} \end{array}\right]\begin{bmatrix} R \\ \hline Y \end{bmatrix} = \begin{bmatrix} 0 \\ \hline 0 \end{bmatrix} \end{aligned} \tag{3.39}$$

where

$$M_{v1} = \begin{bmatrix} m_v & 0 \\ 0 & I_v \end{bmatrix}; M_{v2} = \begin{bmatrix} m_1 & 0 \\ 0 & m_2 \end{bmatrix}$$
$$C_{v11} = \begin{bmatrix} C_{s1} + C_{s2} & (-C_{s1}a_1 + C_{s2}a_2)S \\ (-C_{s1}a_1 + C_{s2}a_2)S & (C_{s1}{a_1}^2 + C_{s2}{a_2}^2)S^2 \end{bmatrix};$$
$$C_{v12} = \begin{bmatrix} -C_{s1} & -C_{s2} \\ C_{s1}a_1 S & -C_{s2}a_2 S \end{bmatrix};$$
$$C_{v21} = \begin{bmatrix} -C_{s1} & C_{s1}a_1 S \\ -C_{s2} & -C_{s2}a_2 S \end{bmatrix}; C_{v22} = \begin{bmatrix} C_{s1} & 0 \\ 0 & C_{s2} \end{bmatrix};$$
$$K_{v11} = \begin{bmatrix} K_{s1} + K_{s2} & (-K_{s1}a_1 + K_{s2}a_2)S \\ (-K_{s1}a_1 + K_{s2}a_2)S & (K_{s1}{a_1}^2 + K_{s2}{a_2}^2)S^2 \end{bmatrix};$$
$$K_{v12} = \begin{bmatrix} -K_{s1} & -K_{s2} \\ K_{s1}a_1 S & -K_{s2}a_2 S \end{bmatrix};$$
$$K_{v21} = \begin{bmatrix} -K_{s1} & K_{s1}a_1 S \\ -K_{s2} & -K_{s2}a_2 S \end{bmatrix}; K_{v22} = \begin{bmatrix} K_{s1} & 0 \\ 0 & K_{s2} \end{bmatrix};$$
$$C_t = \begin{bmatrix} C_{t1} & 0 \\ 0 & C_{t2} \end{bmatrix}; K_t = \begin{bmatrix} K_{t1} & 0 \\ 0 & K_{t2} \end{bmatrix};$$
$$Y = \{y_v \quad \theta_v \quad y_1 \quad y_2\}^T.$$

Likewise Eq. (3.39), using Eq. (3.38) in the equation of motion of bridge Eq. (3.33), the equilibrium of the bridge degrees of freedom can be written as:

$$\left[\begin{array}{c|cc} M_b & 0 & 0 \\ \hline 0 & 0 & 0 \\ 0 & 0 & 0 \end{array}\right]\left[\begin{matrix}\ddot{R} \\ \ddot{Y}\end{matrix}\right] + \left[\begin{array}{c|cc} C_b + H_c C_t H_c^T & 0 & -H_c C_t \\ \hline 0 & 0 & 0 \\ 0 & 0 & 0 \end{array}\right]\left[\begin{matrix}\dot{R} \\ \dot{X}\end{matrix}\right]$$
$$+ \left[\begin{array}{c|cc} K_b + H_c K_t H_c^T + H_c C_t v \frac{\partial H_c^T}{\partial x} & 0 & -H_c K_t \\ \hline 0 & 0 & 0 \\ 0 & 0 & 0 \end{array}\right]\left[\begin{matrix}R \\ Y\end{matrix}\right] = \left[\begin{matrix}H_c M_s \\ 0\end{matrix}\right] \tag{3.40}$$

where

$$M_s = \begin{Bmatrix} (m_1 + a_2 m_v)g \\ (m_2 + a_1 m_v)g \end{Bmatrix}.$$

By combining Eq. (3.39) and Eq. (3.40), the global equation of motion of vehicle-bridge interaction system becomes:

$$\left[\begin{array}{c|cc} M_b & 0 & 0 \\ \hline 0 & M_{v1} & 0 \\ 0 & 0 & M_{v2} \end{array}\right]\left[\begin{matrix}\ddot{R} \\ \ddot{Y}\end{matrix}\right] + \left[\begin{array}{c|cc} C_b + H_c C_t H_c^T & 0 & -H_c C_t \\ \hline 0 & C_{v11} & C_{v12} \\ -C_t H_c^T & C_{v21} & C_{v22} \end{array}\right]\left[\begin{matrix}\dot{R} \\ \dot{Y}\end{matrix}\right]$$
$$+ \left[\begin{array}{c|cc} K_b + H_c K_t H_c^T + H_c C_t v \frac{\partial H_c^T}{\partial x} & 0 & -H_c K_t \\ \hline 0 & K_{v11} & K_{v12} \\ -K_t H_c^T - C_t v \frac{\partial H_c^T}{\partial x} & K_{v21} & K_{v22} \end{array}\right]\left[\begin{matrix}R \\ Y\end{matrix}\right] = \left[\begin{matrix}H_c M_s \\ 0\end{matrix}\right] \tag{3.41}$$

The Eq. (3.41) is the vehicle-bridge interaction equation, and the Eq. (3.37) is the front and rear axle load equations which are compose of static load of vehicle and dynamic interaction force between vehicle and bridge. The vehicle-bridge interaction equation can be solved step-by-step using either direct integration method such as Newmark's method – average acceleration.

3.3 Force identification using acceleration response

The average acceleration discrete algorithm for force identification has been investigated by Ding et al. (2013). However the proposed method was used only for structures subjected to seismic excitations in numerical simulations and simple laboratory tests. The method has not been tested for real structures or for different type of loading. In this chapter the average acceleration discrete algorithm is extended to axle loads identification of vehicle moving on the bridge deck.

3.3.1 System equations of motion

Considering a bridge under a moving vehicle, the equations of motion of the bridge beam can be expressed by

$$M\ddot{x}(t) + C\dot{x}(t) + Kx(t) = L(t)F(t) \tag{3.42}$$

where

M, C, K –the mass, damping and stiffness matrices of the bridge

$F(t)$ – vehicle-bridge interaction force vector with respect to number of axles

$L(t)$ – the global load transformation matrix, transformation external loads to nodal loads for each time step, the matrix with zero entries except at the degrees of freedom corresponding to the nodal displacements of the beam elements on which the load is acting

3.3.2 Discrete equation

The equations of motion of structural system form the continuous system equations which can be transformed into the equivalent discrete equations. The superscripts C and D denote the matrices for continuous and discrete system respectively. Recall the Eq. (3.42) and rearrange into the state-space expression, the continuous system equations become

$$\dot{z}(t) = A^C z(t) + B^C(t)F(t) \tag{3.43}$$

where

$$z(t) = \begin{bmatrix} x(t) \\ \dot{x}(t) \end{bmatrix}$$

$$A^C = \begin{bmatrix} 0 & I \\ -M^{-1}K & -M^{-1}C \end{bmatrix}$$

$$B^C(t) = \begin{bmatrix} 0 \\ M^{-1}L(t) \end{bmatrix}$$

A^C – continuous system matrix,

$B^C(t)$ – time-varying input matrix due to the moving loading,

I – identity matrix.

After solving above equations, the state $z(t)$ and $\dot{z}(t)$ are known. Then the bridge accelerations at any location can be obtained from the output vector $y(t)$:

$$y(t) = R\ddot{x}(t) \tag{3.44}$$

where

R - output influence matrix for the measured acceleration, which depends on the sensor location information, $R \in R^{m \times ndof}$

m - dimension of the measured responses equal to the number of accelerometers placed on the bridge deck

$ndof$ - number of DOFs of the bridge

This output vector can be alternatively calculated from

$$y(t) = C^C z(t) + D^C(t)F(t) \tag{3.45}$$

where the continuous output matrices are

$$C^C = [RM^{-1}K \quad -RM^{-1}C]$$
$$D^C = RM^{-1}L(t)$$

Due to the fact that actual measured acceleration data is in a discrete form, the above continuous state equations have to be converted into the discrete equations as

$$z(j+1) = A^D z(j) + B^D(j)F(j) \tag{3.46}$$

$$y(j) = C^D z(j) + D^D(j)F(j) \tag{3.47}$$

where

$z(t)$, $y(j)$ and $F(j)$ - respectively the discrete vectors of state, output and load at time step $t = j\Delta t$ for $j = 1,2,\dots,N$

$C^D = C^C$, $D^D = RM^{-1}L(j)$ - discrete system matrices;

A^D, B^D - discrete system matrices which are determined by average acceleration algorithm for load identification at paragraph 3.3.3.

For zero initial conditions, the discrete output becomes the summation of the history load effects as

$$y(j) = \sum_{k=0}^{j} H_k^D \cdot L_{j-k} \cdot F(j-k) \tag{3.48}$$

$F(k)$ – history load vector for $k = 0,1,2,\dots,j$.

3.3.3 Average acceleration algorithm for force identification

The method is based on Newmark- β with the following assumptions:

$$\dot{x}_{k+1} = \dot{x}_k + \left(\frac{\ddot{x}_k + \ddot{x}_{k+1}}{2}\right)\Delta t \tag{3.49}$$

$$x_{k+1} = x_k + \dot{x}_{k+1}\Delta t + \left(\frac{\ddot{x}_k + \ddot{x}_{k+1}}{4}\right)\Delta t \tag{3.50}$$

Therefore the incremental acceleration and velocity are:

$$\Delta\dot{x} = \dot{x}_{k+1} - \dot{x}_k = 2\frac{\Delta x_k}{\Delta t} - 2\dot{x}_k \tag{3.51}$$

$$\Delta\ddot{x} = \ddot{x}_{k+1} - \ddot{x}_k = 4\frac{\Delta x_k}{\Delta t^2} - 4\frac{\dot{x}_k}{\Delta t} - 2\ddot{x}_k \tag{3.52}$$

By substituting these increments into the equation of motion at any step $(k+1)^{th}$ one can obtain:

$$\left(\frac{4}{\Delta t^2}M+\frac{2}{\Delta t}C+K\right)\Delta x_k = F_{k+1}+M\ddot{x}_k+\left(C+\frac{4}{\Delta t}M\right)\dot{x}_k-Kx_k \tag{3.53}$$

The incremental displacement and velocity can be expressed as:

$$\Delta x_k = \left(\frac{4}{\Delta t^2}M+\frac{2}{\Delta t}C+K\right)^{-1}\left(F_{k+1}+M\ddot{x}_k+\left(C+\frac{4}{\Delta t}M\right)\dot{x}_k-Kx_k\right) \tag{3.54}$$

$$\Delta x_k = \left(\frac{4}{\Delta t^2}M+\frac{2}{\Delta t}C+K\right)^{-1}\left(F_{k+1}+F_k+\frac{4}{\Delta t}M\dot{x}_k-2Kx_k\right) \tag{3.55}$$

$$\Delta\dot{x}_k = \dot{x}_{k+1}-\dot{x}_k = 2\frac{\Delta x_k}{\Delta t}-2\dot{x}_k = 2\frac{1}{\Delta t}\left(\frac{4}{\Delta t^2}M+\frac{2}{\Delta t}C+K\right)^{-1} \cdot\left(F_{k+1}+F_k+\frac{4}{\Delta t}M\dot{x}_k-2Kx_k\right)-2\dot{x}_k \tag{3.56}$$

The displacement and velocity at time step $(k+1)^{th}$ can be written as:

$$\begin{bmatrix}x_{k+1}\\ \dot{x}_{k+1}\end{bmatrix} = \begin{bmatrix}x_k+\Delta x\\ \dot{x}_k+\Delta\dot{x}\end{bmatrix} \tag{3.57}$$

or

$$z_{k+1} = A^D z_k + B^D L_k \cdot F_k \tag{3.58}$$

where

$$z_{k+1} = \begin{bmatrix}x_{k+1}\\ \dot{x}_{k+1}\end{bmatrix}$$

$$B^D = \begin{bmatrix}\left(\frac{4}{\Delta t^2}M+\frac{2}{\Delta t}C+K\right)^{-1}\\ \frac{2}{\Delta t}\left(\frac{4}{\Delta t^2}M+\frac{2}{\Delta t}C+K\right)^{-1}\end{bmatrix}$$

$$A^D = \begin{bmatrix}I-2\left(\frac{4}{\Delta t^2}M+\frac{2}{\Delta t}C+K\right)^{-1}K & \frac{4}{\Delta t}\left(\frac{4}{\Delta t^2}M+\frac{2}{\Delta t}C+K\right)^{-1}M\\ -\frac{4}{\Delta t}\left(\frac{4}{\Delta t^2}M+\frac{2}{\Delta t}C+K\right)^{-1}K & \frac{8}{\Delta t^2}\left(\frac{4}{\Delta t^2}M+\frac{2}{\Delta t}C+K\right)^{-1}M-I\end{bmatrix}$$

Then the output $y(j)$ can be represented by

$$y(j) = \sum_{k=0}^{j} H_k^D \cdot L_{j-k} \cdot F(j-k) \tag{3.59}$$

$$H_0^D = D^C \tag{3.60}$$

$$H_1^D = C^C B_{j-1}^D \tag{3.61}$$

$$H_k^D = C^C \left(\prod_{i=j-k+1}^{j-1} A_i^D \right) B_{j-k}^D \tag{3.62}$$

The superscript D denotes the system matrix in a new discrete version with average acceleration discrete algorithm.

3.3.4 Iterative regularization method

The general form of the acceleration output as a function of the load input based on average acceleration algorithm (3.59) can be expressed as

$$Y = H_L F \tag{3.63}$$

$$H_L = \begin{bmatrix} H_0 & 0 & \cdots & 0 \\ H_1 & H_0 & \cdots & 0 \\ \vdots & \vdots & \ddots & 0 \\ H_{N-1} & H_{N-2} & \cdots & H_0 \end{bmatrix} L^S \tag{3.64}$$

$$L^S = \begin{bmatrix} L_0 & 0 & \cdots & 0 \\ 0 & L_1 & \cdots & 0 \\ \vdots & \vdots & \ddots & 0 \\ 0 & 0 & \cdots & L_{N-1} \end{bmatrix} \tag{3.65}$$

where

Y – represents the measured acceleration response.

To identify the load vector F from the measured acceleration of the bridge Y, both sides of above equations are pre-multiplied with a pseudo inverse of the matrix H_L. The identified load $\hat{F}$ is obtained by a conventional least-square method as

$$\hat{F} = (H^T H)^{-1} H^T Y \tag{3.66}$$

However above equations become an ill-posed condition when the position of the moving load is close to the bridge supports. The regulation method as proposed by Tikhonov might be employed to obtain the improved solution as

$$\hat{F} = (H^T H + \lambda I)^{-1} H^T Y \tag{3.67}$$

where

λ - non-negative penalty coefficient.

4. Numerical Example

The purpose of this numerical study is to approximate weight of the truck moving over the bridge. The Newmark-β method is employed to obtain acceleration response of the bridge. The average acceleration algorithm is adopted for load identification using only bridge acceleration as the input. Four numerical examples are investigated. In first numerical examples moving vehicle is modeled as a point load. While in the last one it is modeled as the vehicle system with 4 degrees of freedom: vertical displacement, rotation of vehicle mass, vertical displacement of front and rear axle suspension mass.

To study the accuracy of identified force, the relative percentage error is calculated based on force and response.

$$error_F = \frac{\left\|\hat{F} - F_{actual}\right\|}{\|F_{actual}\|} \cdot 100\% \tag{4.1}$$

$$error_{res} = \frac{\left\|\hat{\ddot{x}} - \ddot{x}_{actual}\right\|}{\|\ddot{x}_{actual}\|} \cdot 100\% \tag{4.2}$$

Where $\hat{F}$ and $\hat{\ddot{x}}$ denote the identified load and identified acceleration, respectively.

4.1 System properties

The vehicle-bridge system as in Figure 4.1 is considered. The bridge deck is simplified as a simply supported beam with constant cross-section with properties given in Table 4.1. The vehicle is a 4-degree of freedom system consisting of vertical displacement, rotation of vehicle mass, vertical displacement of front and rear axle suspension mass.

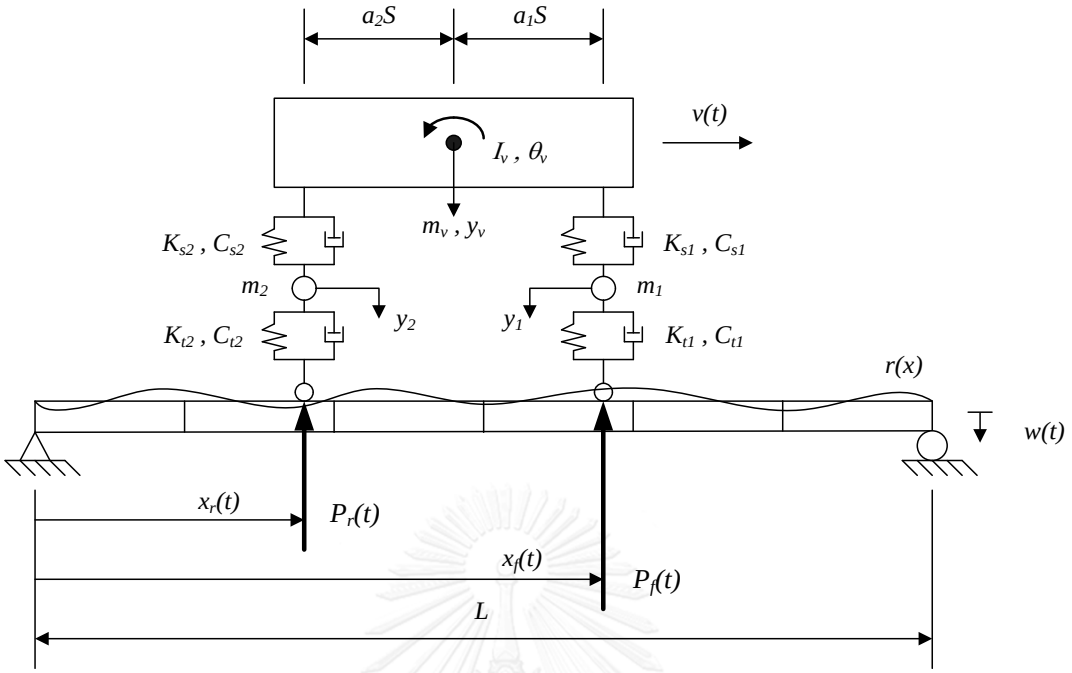

Figure 4.1 Vehicle-bridge system

Table 4.1 Properties of bridge and vehicle

Bridge	Vehicle		
EI=2.3x10^{10} N/m^2	I_v=9.50E5 kg-m^2	m_1 = 700 kg	k_{t2}=3.50·10^6 N/m
L= 36 m	m_v=28780 kg	m_2 = 1100 kg	c_{s1}=1.00·10^4 N/m/s
ς =0.02	S =4.27 m	k_{s1}=0.40·10^6 N/m	c_{s2}=2.00·10^4 N/m/s
ρ =5x10^3 kg/m	a_1 =0.567	k_{s2}=1.00·10^6 N/m	c_{t1}=3.90·10^3 N/m/s
	a_2 =0.433	k_{t1}=1.75·10^6 N/m	c_{t2}=4.30·10^3 N/m/s

4.2 Equivalent SDOF bridge system

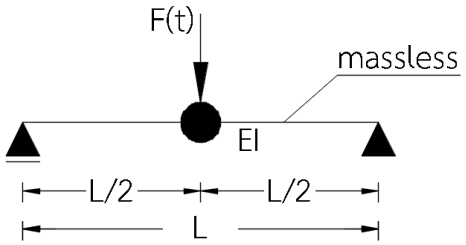

Figure 4.2 Single Degree of Freedom system

The numerical study begins with the simplest system in which the bridge is modeled by single-degree-of-freedom system (SDOF) as in Figure 4.2. The mid-span deflection of the bridge is considered to be the DOF. The properties of this equivalent SDOF are obtained from the first modal properties of the bridge. Four basic load functions F(t) with time-varying amplitude as in Figure 4.3 are investigated with T and tx equal to 1.8 and 0.1 seconds, respectively. The maximum load is equal to F_{max}=200kN. Time step for all simulations is equal to dt=0.0005s.

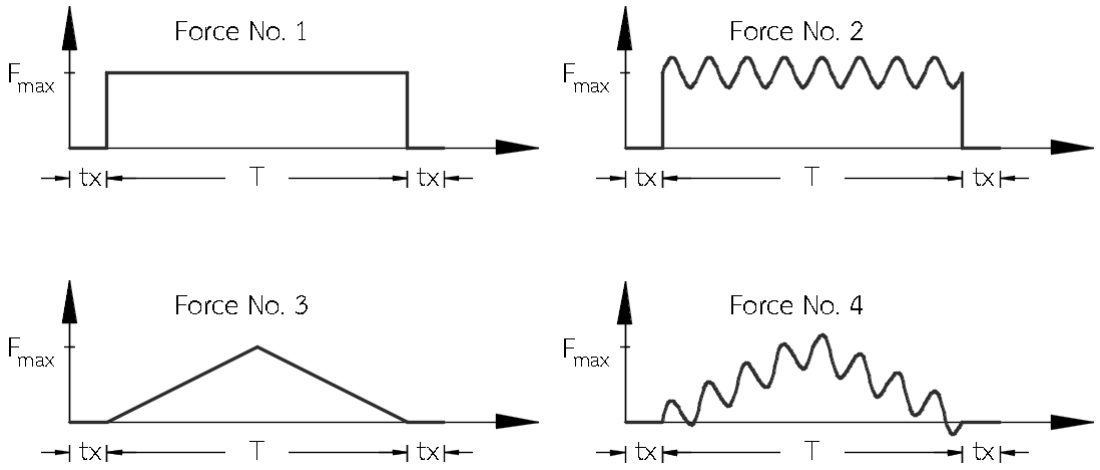

Figure 4.3 Time varying amplitude load functions

The influence of load function on accuracy of the identified force is investigated and shown as in Fig. 4.4.

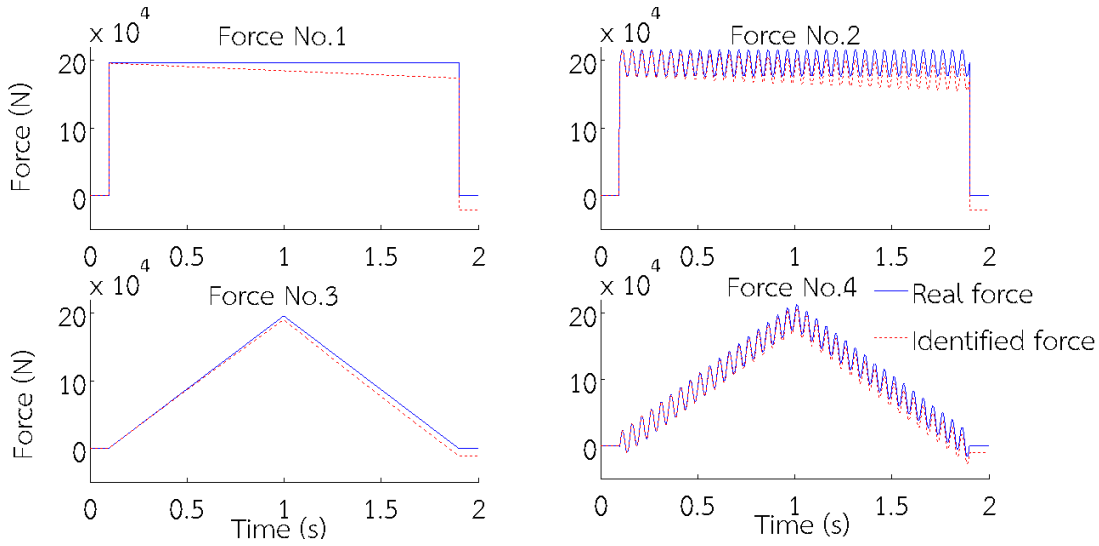

Figure 4.4 Identified forces for Single Degree of Freedom system

Table 4.2 presents force identification errors for all load functions. For different load functions applied to the system, the errors of identified force are found to be less than 10% for all cases.

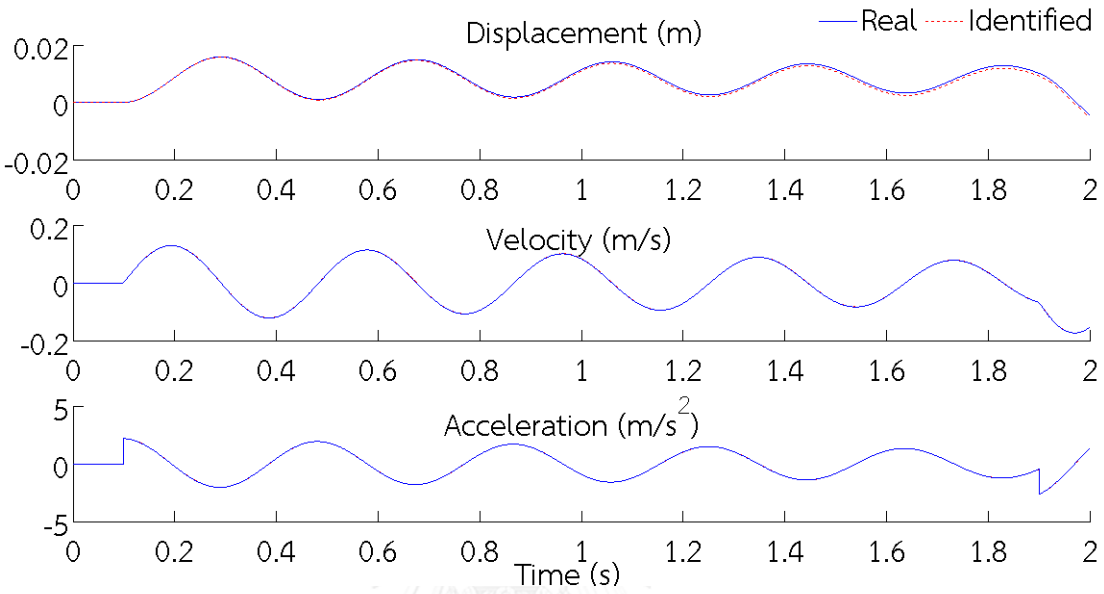

Figure 4.5 Reproduced responses for Force No.1

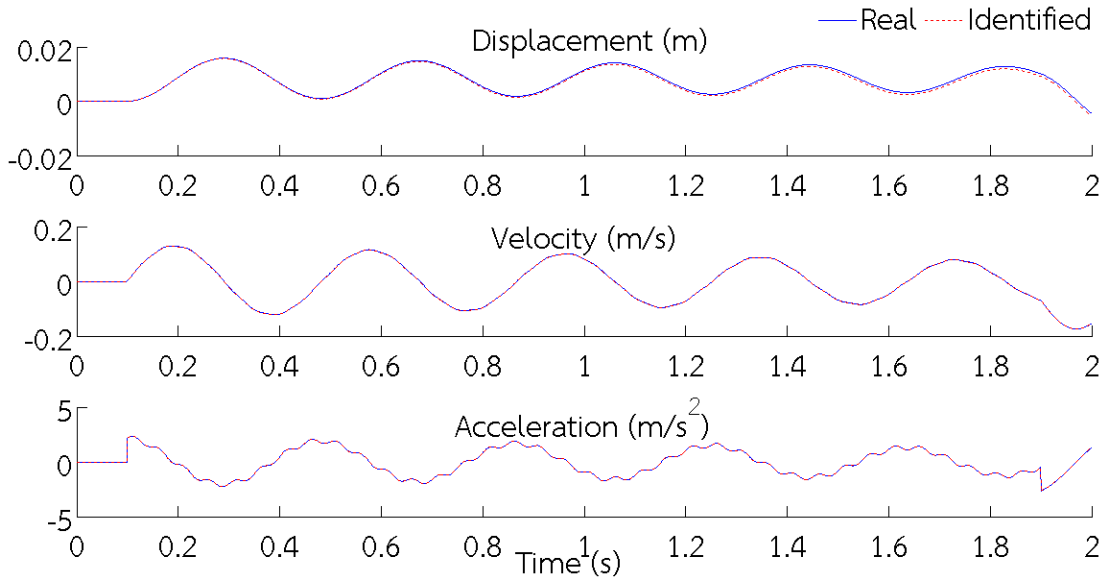

Figure 4.6 Reproduced responses for Force No.2

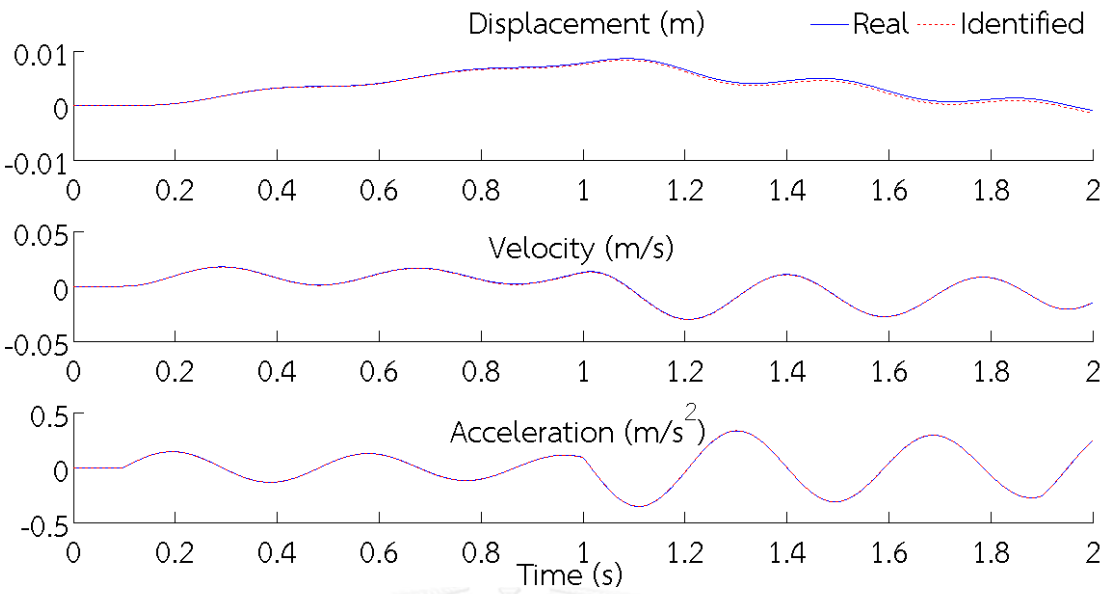

Figure 4.7 Reproduced responses for Force No.3

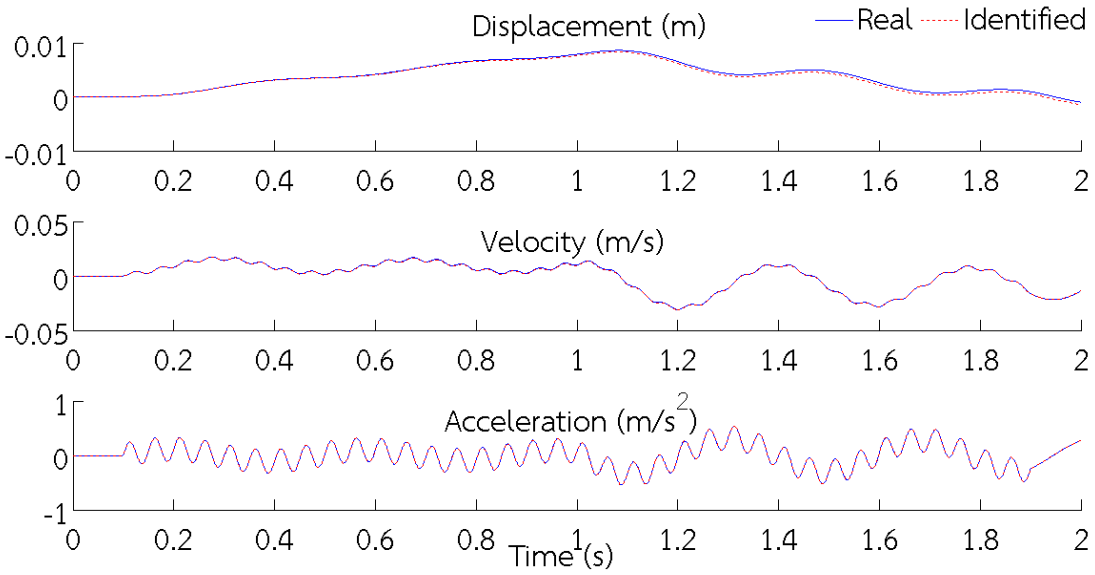

Figure 4.8 Reproduced responses for Force No.4

From table 4.2, the following observations can be made. Even though the average force identification error is 6.87%, the identified responses are rather accurate. In particular the error of acceleration is less than 0.5%. It is also observed that for different loadings similar errors of acceleration and displacement are reported. It can be

concluded that the type of time varying amplitude load function does not influence the accuracy of force identification.

Table 4.2 Identification error for Single Degree of Freedom system

Force	Error[%]			
	F	$\ddot{x}$	$\dot{x}$	x
No.1	7.15	0.43	0.76	6.17
No.2	7.14	0.43	0.76	6.18
No.3	6.62	0.53	2.20	6.50
No.4	6.57	0.40	2.25	6.51
Average	6.87	0.45	1.49	6.34

In addition, the errors between load and displacement identifications are noticed to be in the same order. The reason of this relation could be following. In the proposed method, the acceleration response is an input data which is used to estimate the dynamic force of the system. Since dynamic force depends not only on acceleration, but also displacement and velocity response, the other responses have to be approximated from acceleration. To obtain these two responses, double integration of acceleration is indirectly made.

The error of approximation of velocity is a constant that is added to the function, obtained by evaluating the integral of a given function of acceleration. The error of approximation of displacement becomes a linear function of time. Since the part of identified force, which relies on the displacement, is the most important, the accuracy of identification relies mainly on the accuracy of displacement. The error of approximation of displacement depends on the number of time steps. The higher the number of time steps, the bigger the accumulation of the error. Due to that, the difference between real and identified force increases linearly with the time. It should be noted, that reducing the number of time steps should not be made by enlarging the length of time step, since it will increase the error.

4.3 Bridge with a non-moving load

In this paragraph, Multi Degree of Freedom System is studied. The bridge is modeled by 8 beam elements. The vehicle is simplified as a non-moving force applied in the middle of the beam which is shown in Figure 4.9. Two types of loading, i.e. Force No. 2 and Force No.4, are considered. Time step for all simulations is equal to dt=0.0005s. Three accelerometers are placed on the bridge deck. The location of these accelerometers is shown in Figure 4.10.

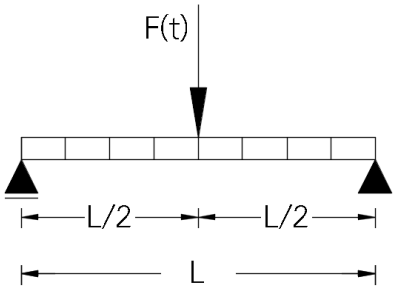

Figure 4.9 MDOF – non-moving load at mid-span

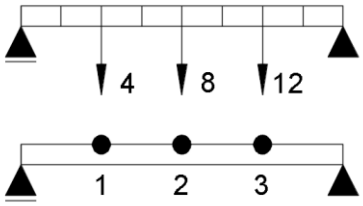

Figure 4.10 Schematic of sensor locations

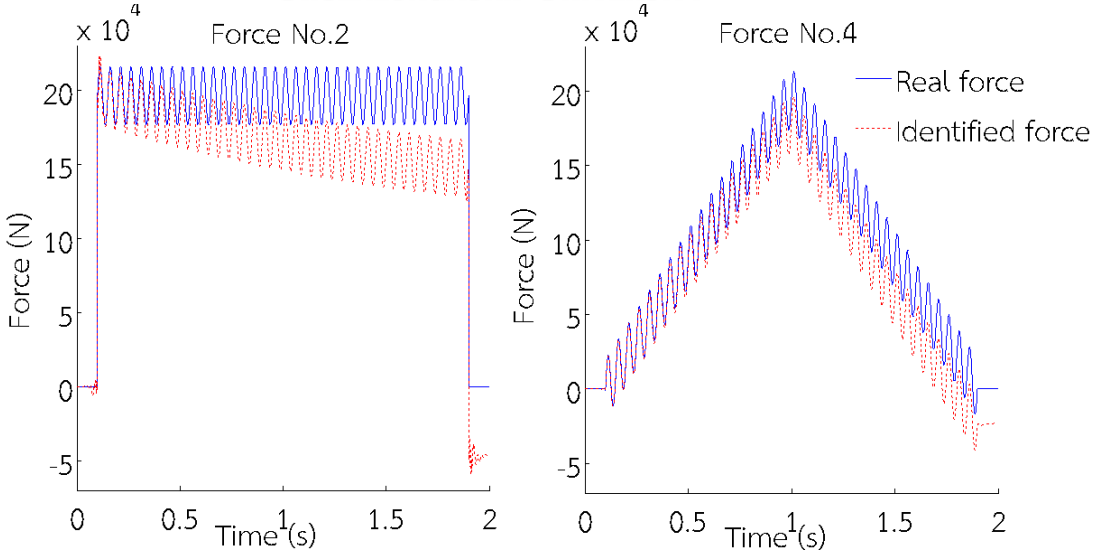

Figure 4.11 Identified forces for MDOF with non-moving load

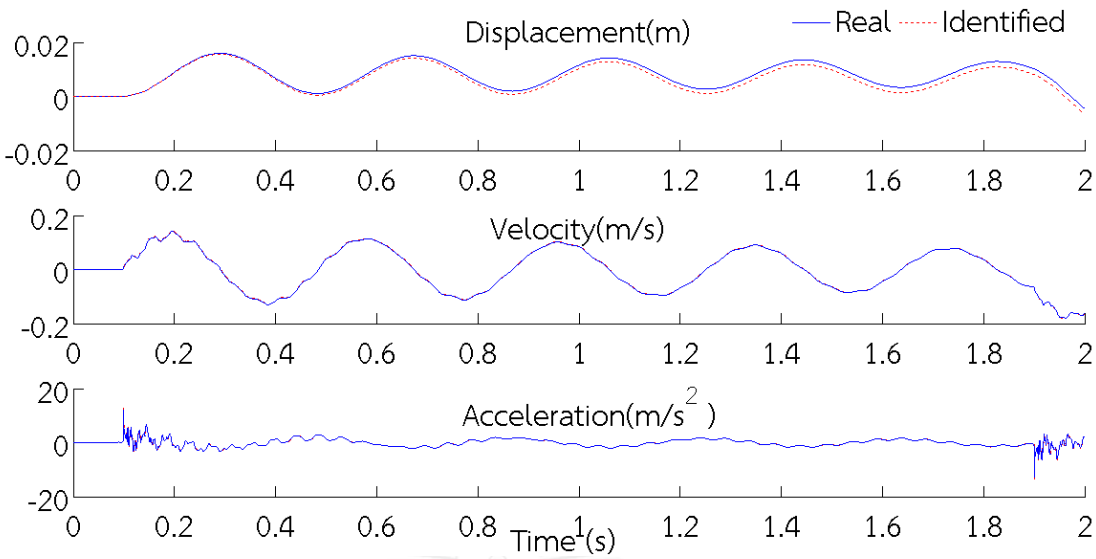

Figure 4.12 Reproduced responses for Force No.2

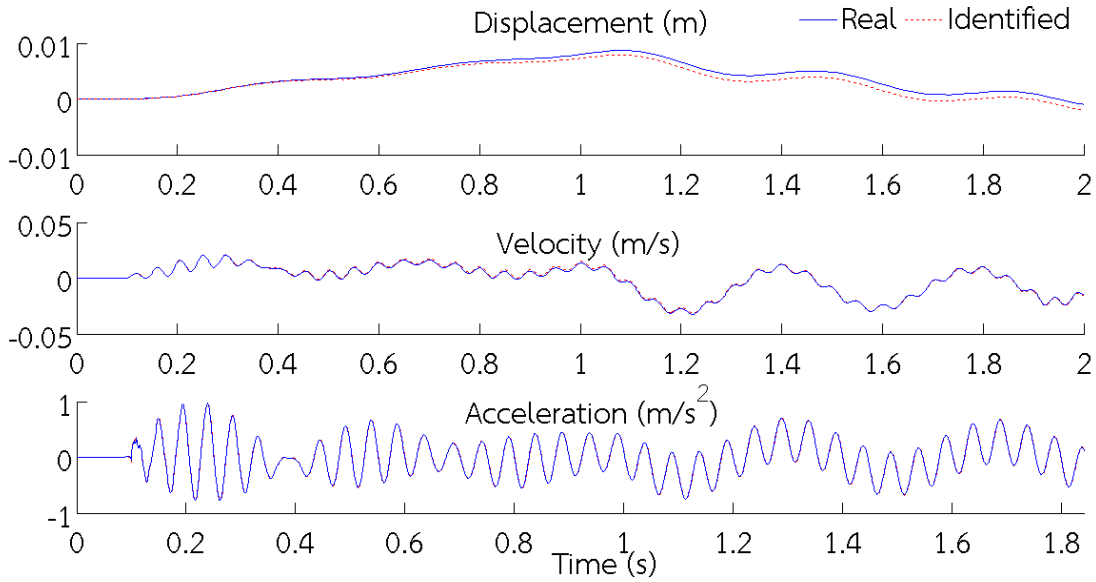

Figure 4.13 Reproduced responses for Force No.4

Table 4.3 Identification error for MDOF system with non-moving load

Force No.	Error[%]			
	F	$\ddot{x}$	$\dot{x}$	x
2.	17.35	8.78	1.60	15.05
4.	16.52	4.71	5.92	16.37
Average	16.94	6.75	3.76	15.71

For the same load functions applied to the SDOF system and MDOF system, the error of force identification is significantly different. For MDOF system with non-moving force the average error is 16.94%, which is more than 2 times higher than that for SDOF. The increase in error of force identification might be caused by imperfections of the model. Using more complicated model with higher number of degrees of freedom causes difficulties in capturing the real behavior of the system.

Similar linearly increasing error between identified force and real force and the relation between errors of displacement and force are observed. The errors are larger due to the use of more complicated model.

The type of load function does not influence the accuracy of identified force as it was for SDOF. However the decrease in the accuracy of acceleration reproduction can be observed. It seems that for continuous load function, the accuracy of reproduced acceleration is higher for MDOF systems. These obtained results imply that the load identification demands higher mode information to accurately reproduce the acceleration response.

4.4 Bridge with a moving load

This section considers MDOF system with a concentrate load moving over the beam. The time-varying amplitude load function as in Figure 4.14 is applied. The maximum load is equal to F_{max}=200kN. The system is studied for three different speeds of moving loads which are 10, 20 and 40 m/s, with the excitation frequencies of 62.83, 125.66 and 251.33 rad/s, respectively. The bridge is modeled by 8 beam elements. Time step for all simulations is equal to dt=0.0005s. Three accelerometers are placed on the bridge deck at the same locations as described in paragraph 4.3.

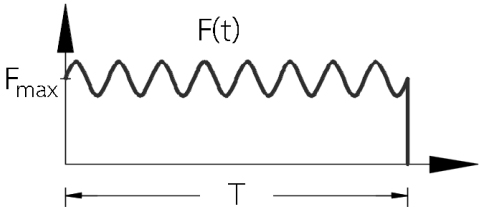

Figure 4.14 Time-varying amplitude load function

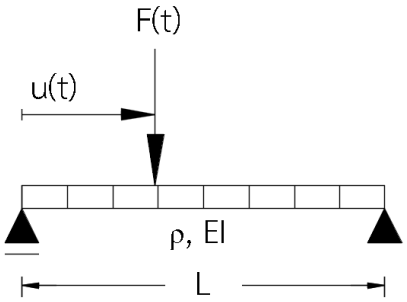

Figure 4.15 MDOF – moving load at mid-span

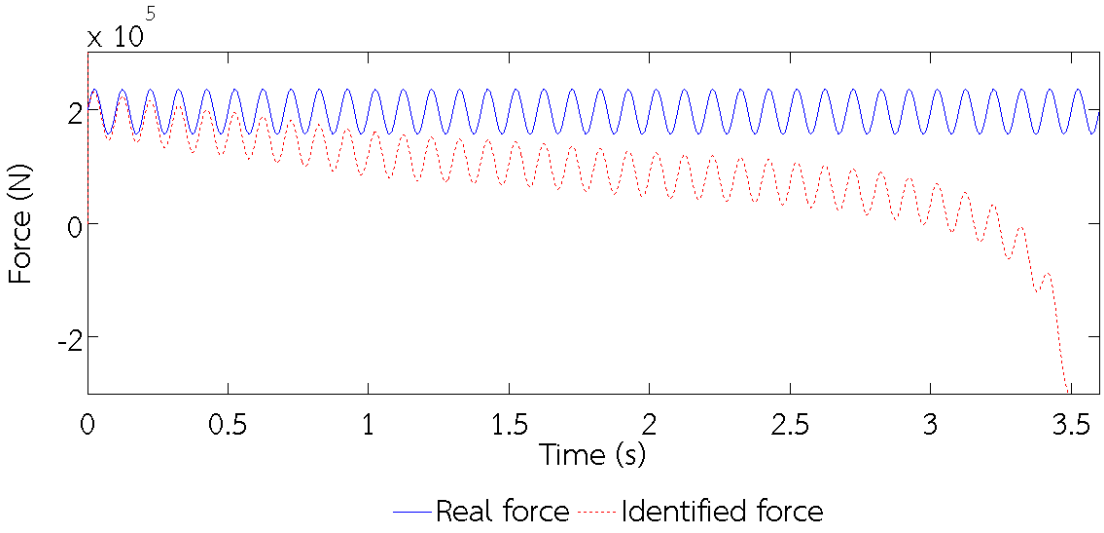

Figure 4.16 Identified force for MDOF with moving load (V=10m/s)

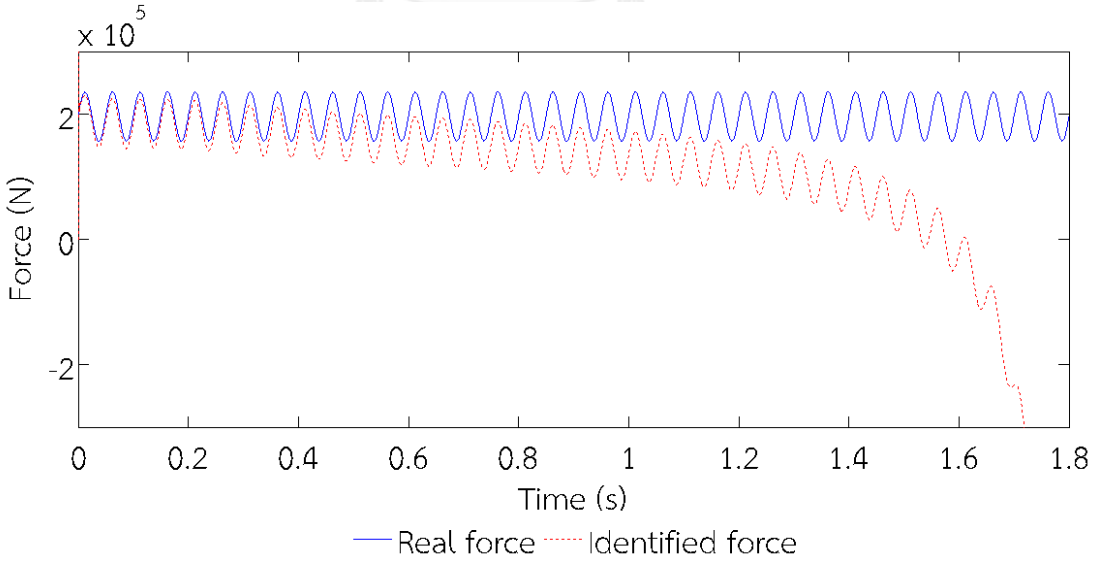

Figure 4.17 Identified force for MDOF with moving load (V=20m/s)

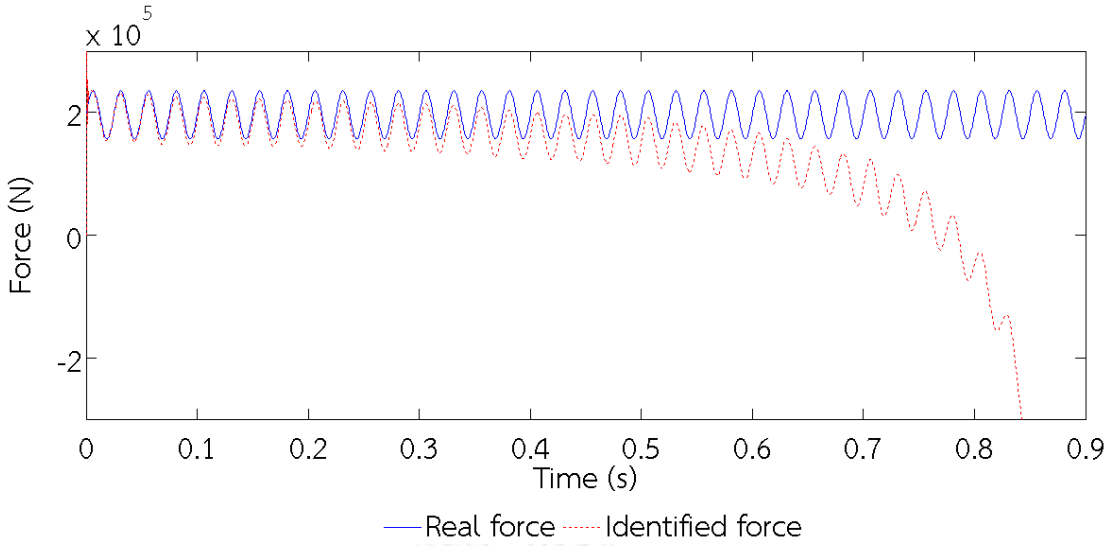

Figure 4.18 Identified force for MDOF with moving load (V=40m/s)

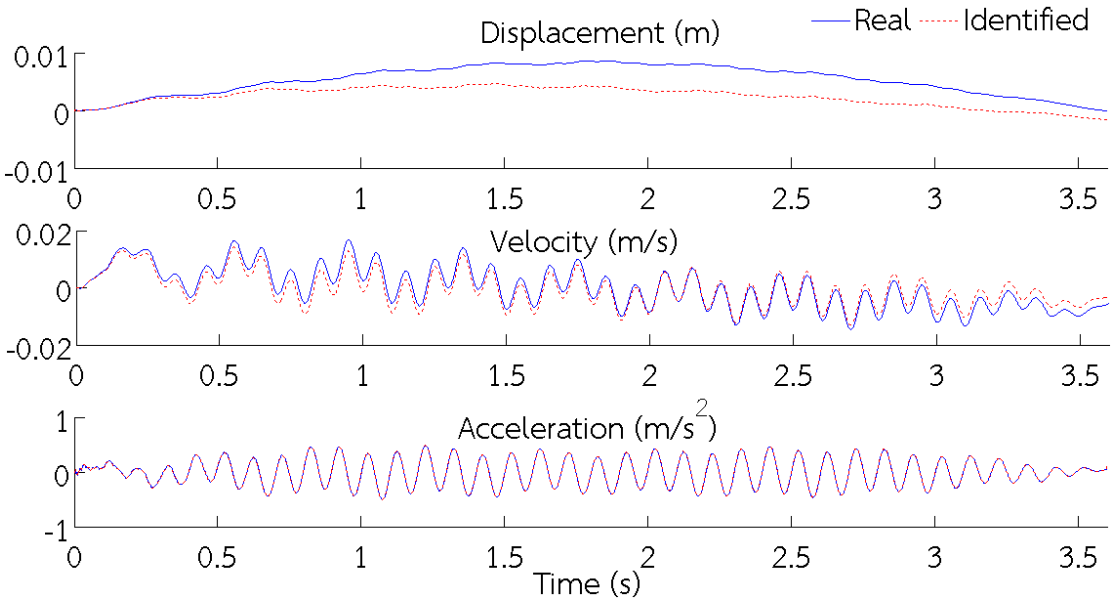

Figure 4.19 Identified responses at mid-span for MDOF with moving load (V=10m/s)

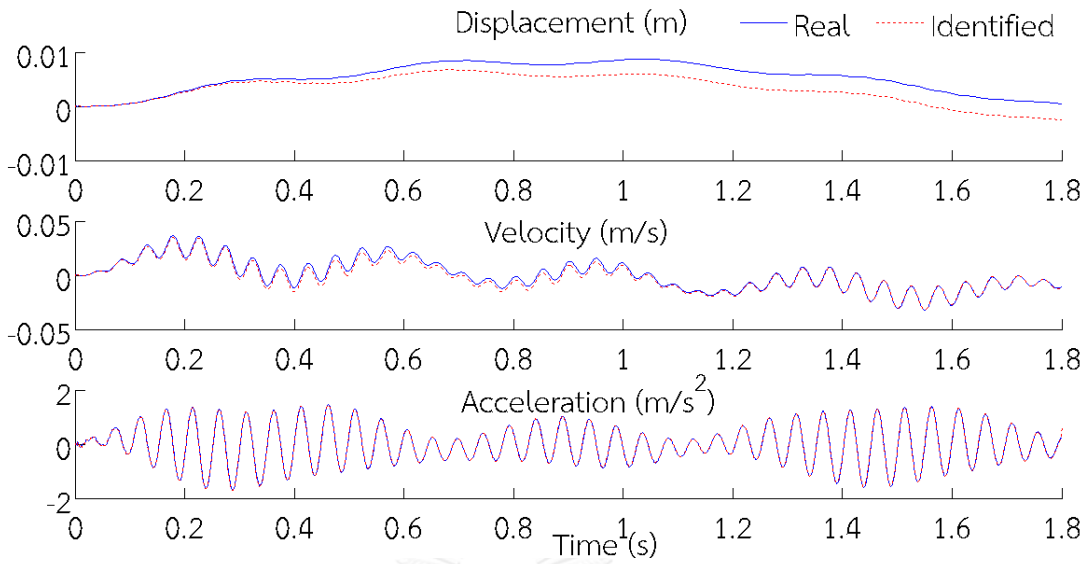

Figure 4.20 Identified responses at mid-span for MDOF with moving load (V=20m/s)

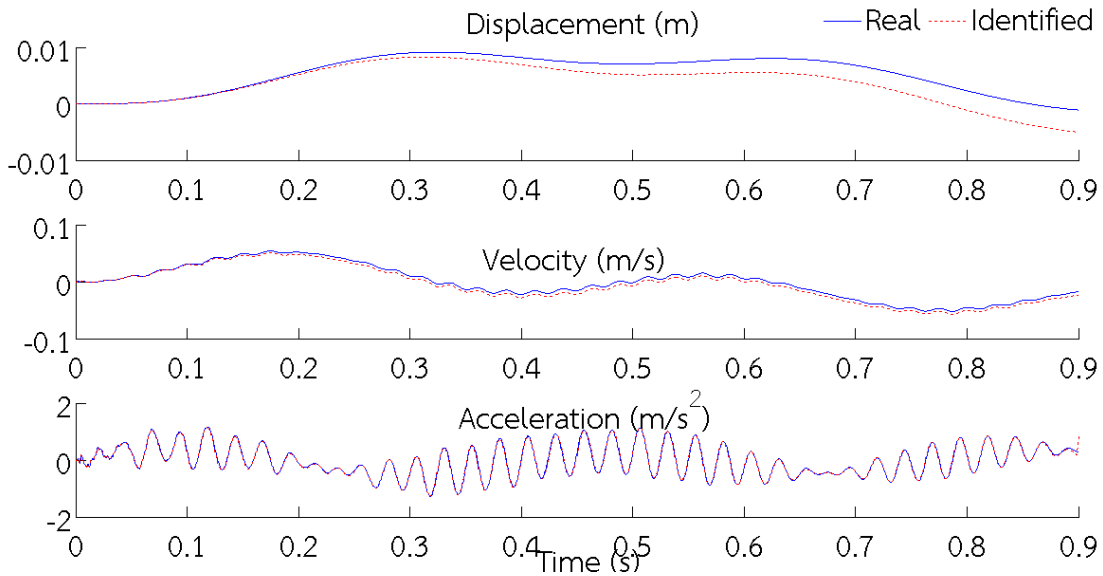

Figure 4.21 Identified responses at mid-span for MDOF with moving load (V=40m/s)

Table 4.4 Percentage error for MDOF system with moving load for different speeds

Speed [m/s]	Error [%]			
	F	$\ddot{x}$	$\dot{x}$	x
10	>100	2.45	33.62	54.88
20	>100	3.69	16.18	38.21
40	>100	7.82	16.07	33.77
Average	>100	4.65	21.96	42.29

Table 4.4 presents the identification errors from three cases of speeds of moving load. Unlike the previous cases, even though the identification errors of the acceleration are found well within 10%, the errors of identified loads are greater than 100% in all cases. This is due to the fact that the system equation becomes an ill-posed condition when the position of moving load is close to the bridge supports. The speed of vehicle influences the accuracy of reproduction of responses. If speed increases, error of reproduced acceleration increases, while error of displacement and velocity decrease.

As shown in Figures 4.17 and 4.20, the similar error between real and identified force and displacement can be observed. It proves that the significant factor in accuracy is error of displacement approximation in force identification, which accumulates with time.

It should be noted that, to improve the identification accuracy, one might reduce the time step size of 0.0005 second to smaller size. However, this seems impractical since it costs on both hardware and software. In the next chapter, to reduce the error due to ill-posed condition, the regularization parameter λ will be applied.

4.5 Bridge with a moving vehicle

This section considers MDOF system with vehicle moving over the beam. The bridge is modeled by 36 beam elements for response simulation and 4 beam elements for force

identification. Three accelerometers are placed on the bridge deck. The location of these accelerometers is shown below.

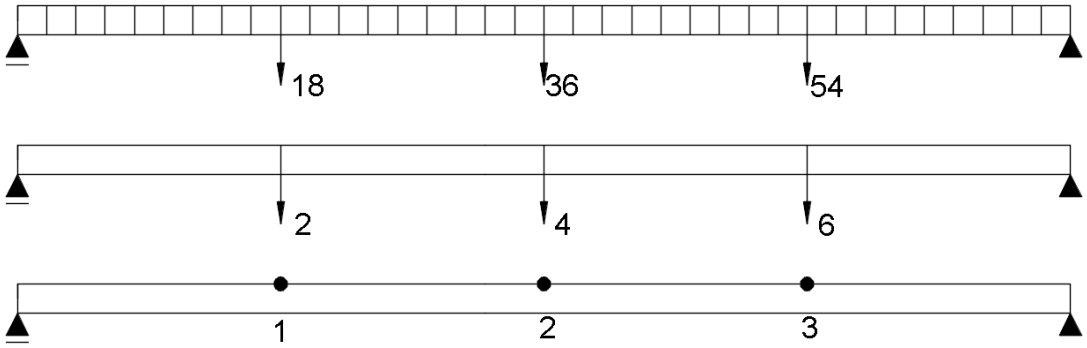

Figure 4.22 Schematic of sensor locations

Table 4.5 Sensor location (DOF no.)

Sensor No.	Simulation	Force identification
1	18	2
2	36	4
3	54	6

For all simulations time step is equal to dt=0.001s and the regularization parameter $\lambda = 10^{-15}$ as in Eq. 3.67. In this numerical study, the 1st part will be focused on the identification of dynamic force for whole time period. While in the 2nd part, weight estimation will be addressed. In these two parts the influence of properties of vehicle on accuracy of force identification will be shown, such as: axle spacing, mass of vehicle and speed.

4.5.1 Dynamic force identification

This section considers identification of dynamic force of moving vehicle over the bridge deck. To demonstrate the accuracy of the identified force, percentage errors, between identified force and real interaction force of front axle, rear axle and summation of two axles, are calculated. In addition, the dynamic structural responses are reproduced using Newmark-β method. The reproduced displacement, velocity and

acceleration at the mid-span of the bridge are plotted and compared with the real forces and bridge responses.

4.5.1.1 Axle spacing

The properties of the vehicle are following: static weight of axles N_t= 300kN, additional force F_{add}= 10%, speed v=20m/s. Three axle spacing are investigated: 0.5S, 1.0S and 1.5S, where S= 4.27m.

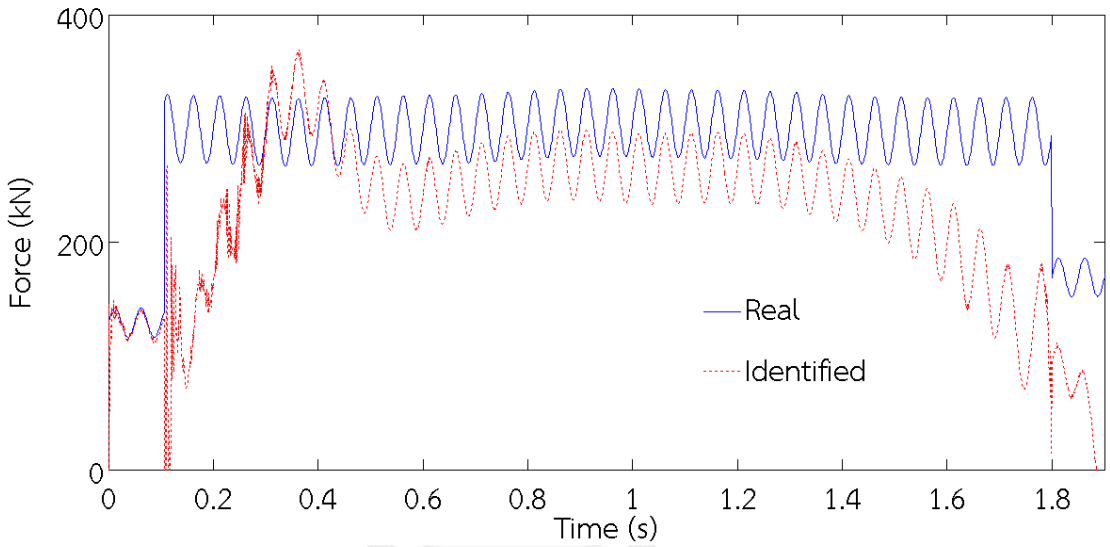

Figure 4.23 Summation of identified forces for 0.5S

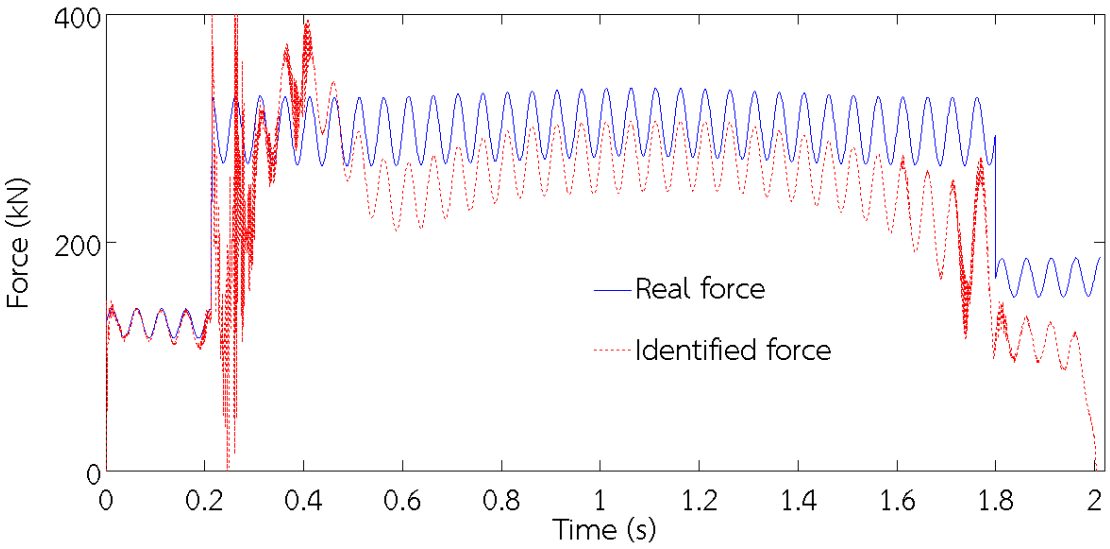

Figure 4.24 Summation of identified forces for 1.0S

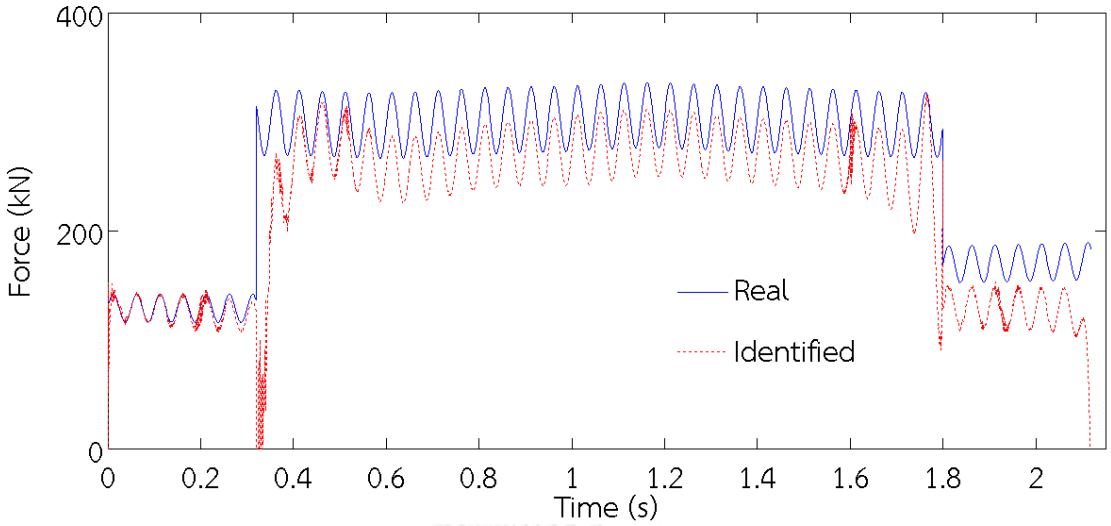

Figure 4.25 Summation of identified forces for 1.5S

The errors of identification occur at the time when front and rear axles enter and leave the bridge deck. However for wider axle spacing the errors become smaller. It can be observed that identified force in time goes away from the real dynamic force.

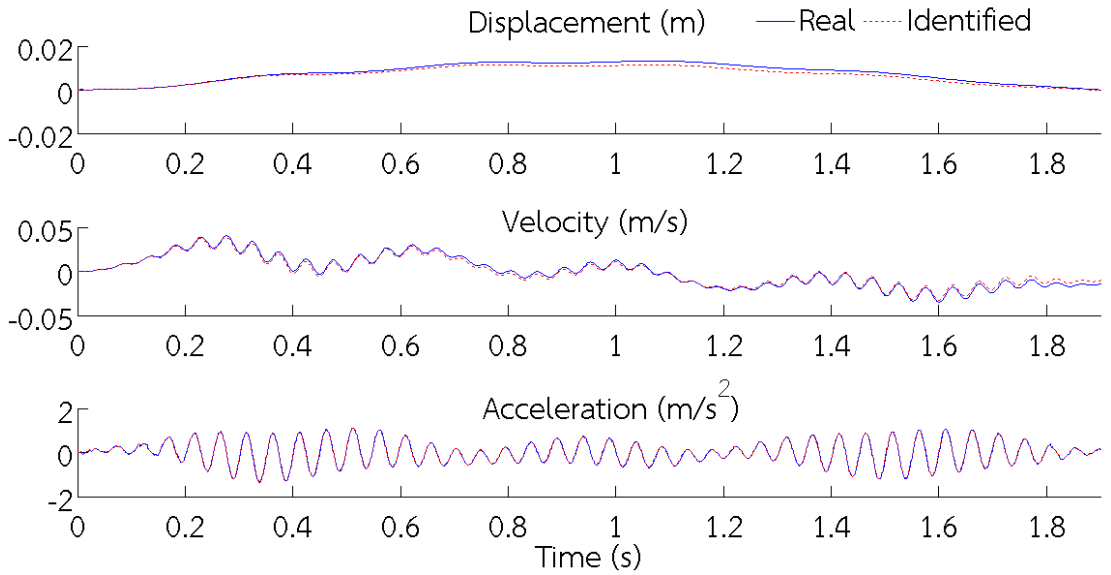

Figure 4.26 Identified responses at mid-span for 0.5S

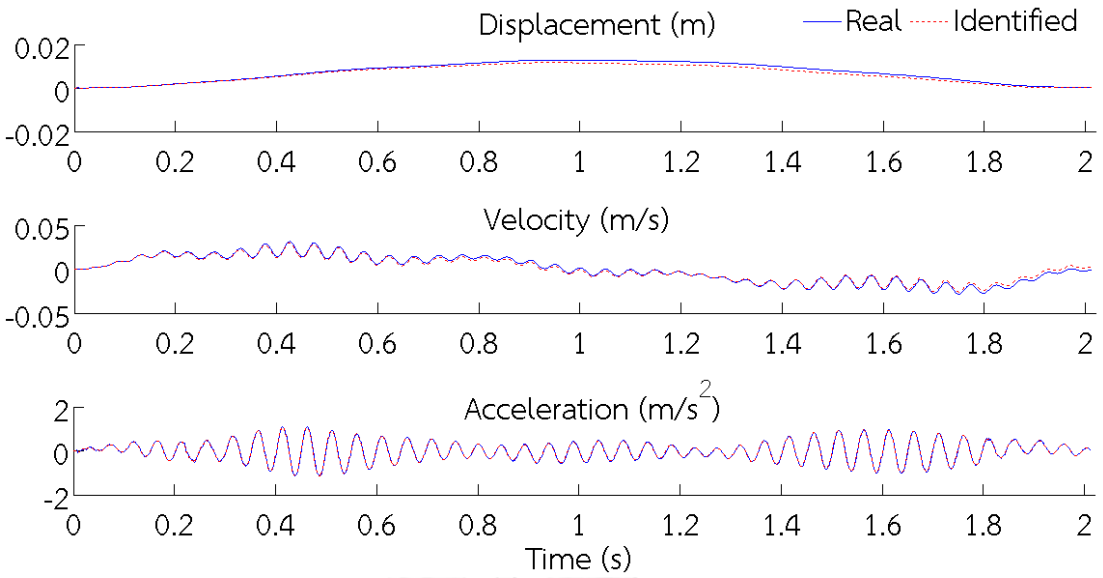

Figure 4.27 Identified responses at mid-span for 1.0S

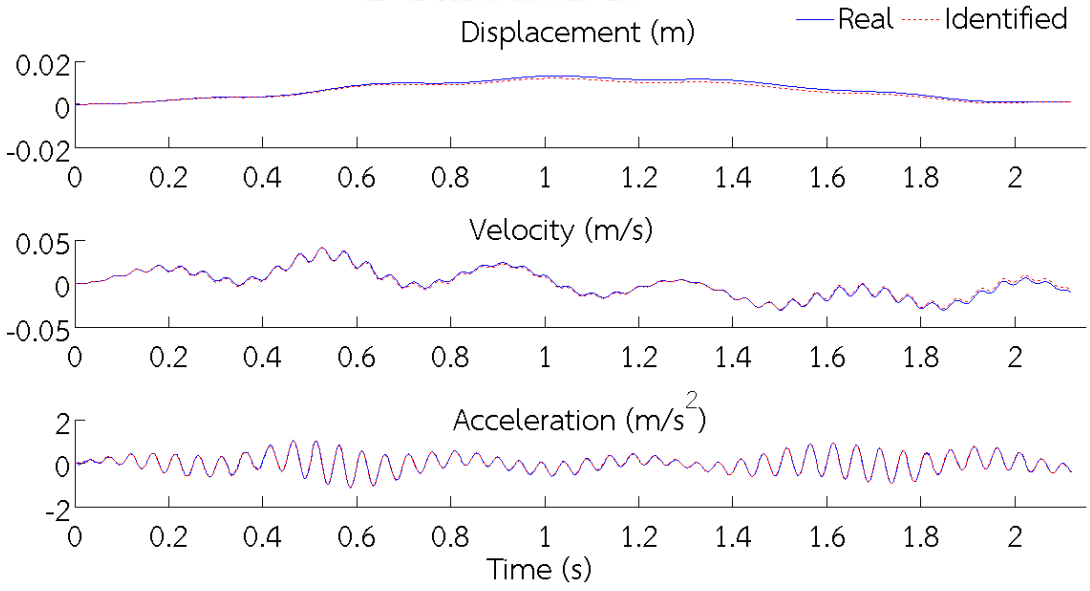

Figure 4.28 Identified responses at mid-span for 1.5S

Table 4.6 Identification error for different axle spacing

Axle spacing	Error[%]					
	Front	Rear	Sum	$\ddot{x}$	$\dot{x}$	x
0.5S	78.33	79.86	30.91	7.27	12.95	13.76
S	38.20	49.75	21.37	7.37	11.94	11.47
1.5S	18.14	35.07	17.89	6.96	9.82	10.68

As shown in Table 4.6, the force identification error decreases as the axle spacing is wider. It seems that summation of dynamic forces of both axles is the most accurate and the least susceptible to the varying of axle spacing. The second most accurate identified value is dynamic force of front axle. It is important to highlight that even though the force identification errors are significant, the reproduced acceleration response is accurate: error is only around 7%. It can be concluded that for significantly different forces, it is possible to obtain very similar responses.

The identified force is prone to varying of axle spacing, while the accuracy of reproduced responses is similar for different axle spacing. The difference between 0.5S and 1.5S is less than 3% for all responses.

For wider axle spacing, the identified force is more accurate. The reason of this relation is connected with the error of displacement approximation. When the displacement is close to zero, the error is smaller. While the axle spacing is wider, the time when only one force is moving over the bridge is longer. This results in simpler model, similar to one point load moving over the bridge which yields smaller error in displacement approximation.

4.5.1.2 Mass of vehicle

The properties of the vehicle are following: axle spacing S= 4.27m and speed v=20m/s. Five static weight are investigated: N_t=100, 200, 300, 400 and 500kN with three different additional force: F_{add}=0, 10 and 20%.

Figures 4.29, 4.30 and 4.31 present the typical comparison of identified with real summation of forces with N_t=500 kN and F_{add}=0, 10 and 20%, respectively.

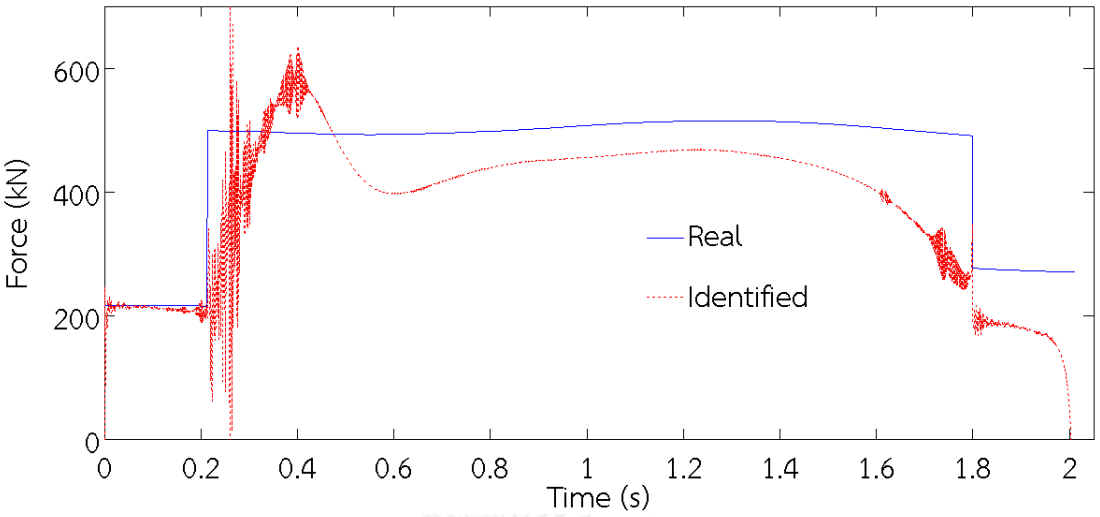

Figure 4.29 Summation of identified forces for N_t=500kN, F_{add}=0%

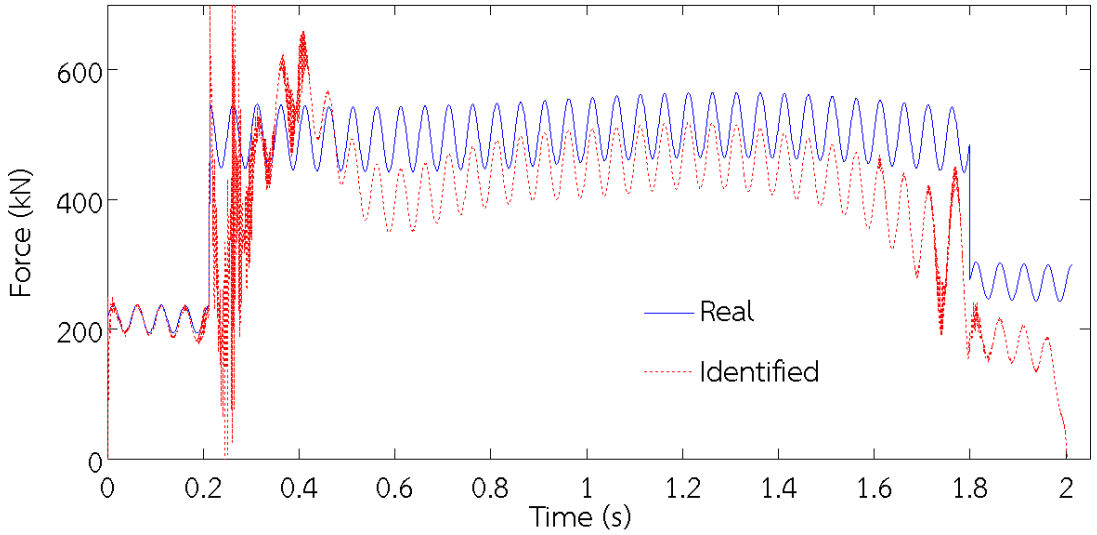

Figure 4.30 Summation of identified forces for N_t=500kN, F_{add}=10%

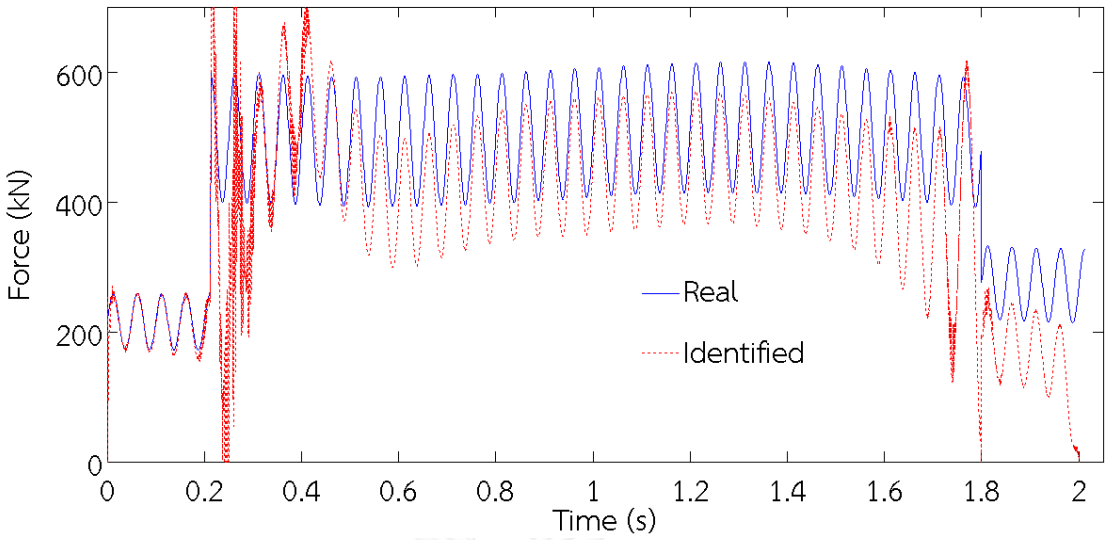

Figure 4.31 Summation of identified forces for N_t=500kN, F_{add}=20%

Table 4.7 Identification error for N_t = 100kN

F_{add}	Error[%]					
	N_t = 100kN					
	Front	Rear	Sum	$\ddot{x}$	$\dot{x}$	x
0	39.95	49.56	21.98	13.19	12.32	11.44
10%	38.72	49.73	21.27	7.37	12.04	11.47
20%	39.88	50.87	21.89	7.21	11.42	11.55
Average	39.52	50.05	21.71	9.26	11.93	11.49

Table 4.8 Identification error for N_t = 200kN

F_{add}	Error[%]					
	N_t = 200kN					
	Front	Rear	Sum	$\ddot{x}$	$\dot{x}$	x
0	39.36	49.47	22.00	12.67	12.26	11.44
10%	38.08	49.65	21.30	7.37	11.98	11.50
20%	39.16	50.83	21.93	7.21	11.37	11.56
Average	38.87	49.98	21.75	9.08	11.87	11.50

Table 4.9 Identification error for N_t = 300kN

F_{add}	Error[%]					
	N_t = 300kN					
	Front	Rear	Sum	$\ddot{x}$	$\dot{x}$	x
0	39.50	49.57	22.07	12.67	12.22	11.42
10%	38.20	49.75	21.37	7.37	11.94	11.47
20%	39.22	50.94	22.00	7.21	11.34	11.53
Average	38.97	50.09	21.81	9.08	11.84	11.47

Table 4.10 Identification error for N_t = 400kN

F_{add}	Error[%]					
	N_t = 400kN					
	Front	Rear	Sum	$\ddot{x}$	$\dot{x}$	x
0	39.72	49.67	22.10	12.61	12.15	11.39
10%	38.38	49.86	21.39	7.36	11.89	11.45
20%	39.35	51.06	22.02	7.21	11.30	11.50
Average	39.15	50.20	21.84	9.06	11.78	11.45

Table 4.11 Identification error for N_t = 500kN

F_{add}	Error[%]					
	N_t = 500kN					
	Front	Rear	Sum	$\ddot{x}$	$\dot{x}$	x
0	39.75	49.65	22.07	12.52	12.12	11.39
10%	38.41	49.84	21.36	7.36	11.86	11.44
20%	39.35	51.04	21.98	7.21	11.27	11.50
Average	39.17	50.18	21.80	9.03	11.75	11.44

It is clearly seen from obtained results that the mass of vehicle and additional force do not have any influence on the accuracy of force identification. However, it can be observed that for higher additional force, the reproduced acceleration response is more accurate. It seems that for sinusoidal force is easier to identify acceleration response accurately than for constant force. The reason of this relation is that it is impossible to predict static load using only acceleration response, so for force with dynamic pattern such as sinusoid, the reproduced acceleration is more accurate.

It can be concluded that method of identification is equally accurate for different weights of moving vehicles and different magnitude of bridge roughness.

4.5.1.3 Speed of vehicle

The properties of the vehicle are following: static weight of axles N_t= 300kN, additional force F_{add}= 10%, axle spacing S= 4.27m. The system is studied for eight different speeds of moving which are 5, 10, 15, 20, 25, 30, 35 and 40m/s, with the excitation frequencies of 31.42, 62.83, 94.25, 125.67, 157.08, 188.50, 219.91 and 251.33 rad/s, respectively.

The parameter which represents the effect of the speed- α is introduced by Fryba (1973). The given parameter is a ratio of speed of vehicle to critical speed. The critical speed $v_{cr} = 2Lf_1$ depends on length of the bridge and 1st natural frequency. For the frequency of studied bridge equal to 2.6 Hz, the critical speed is equal to 187.2 m/s. For studied speeds of vehicle such as 5 m/s and 40 m/s, α is equal only to 0.027 and 0.2, respectively. It implies that the effect of the speed is significantly small and that studied vehicle-bridge system is almost a static system. The errors may be caused by the fact that it is not possible to identify static force using only acceleration response.

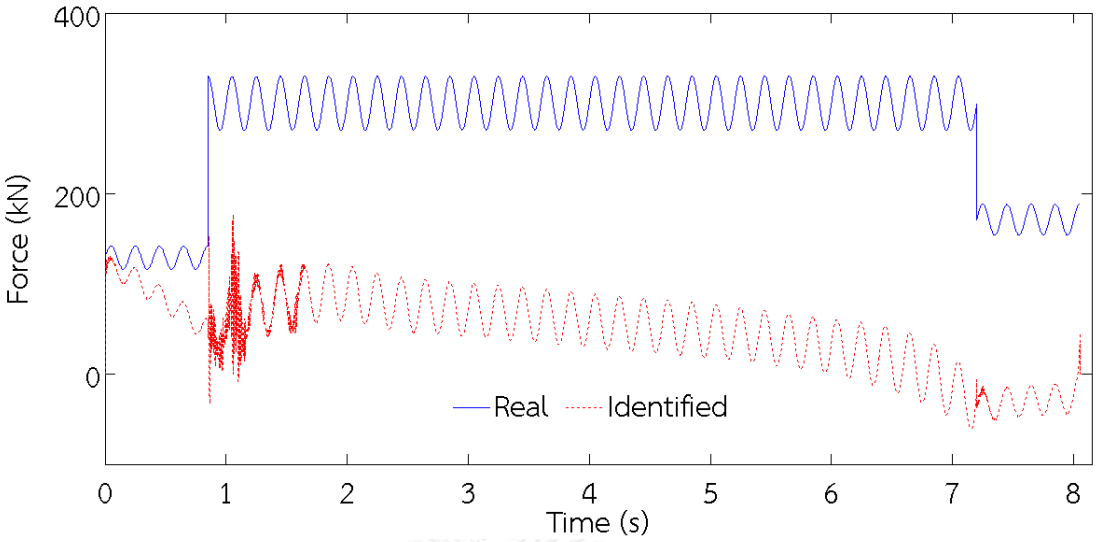

Figure 4.32 Summation of identified forces for v=5m/s

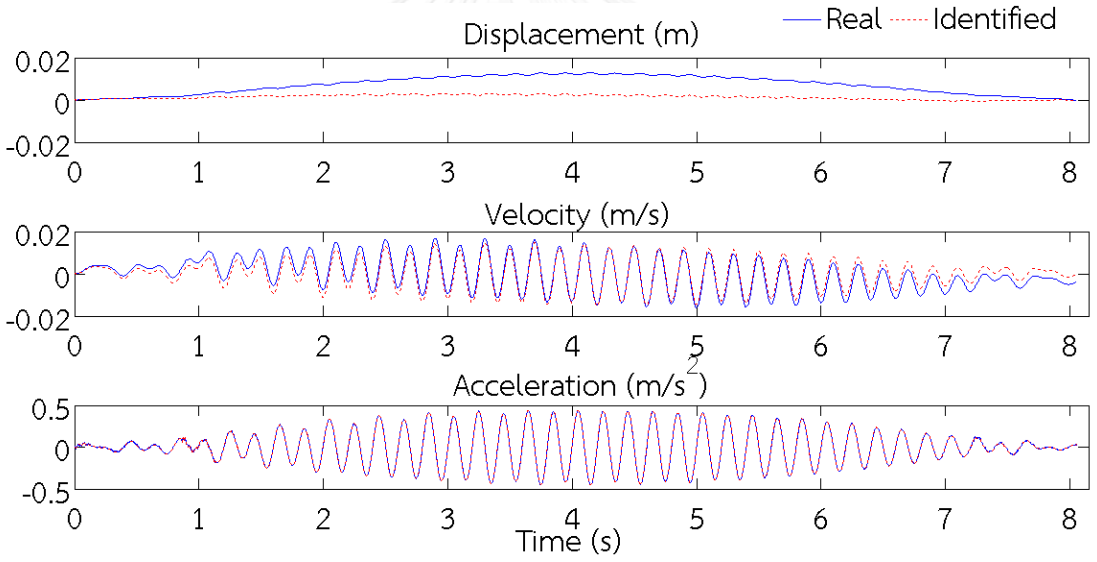

Figure 4.33 Identified responses at mid-span for v=5m/s

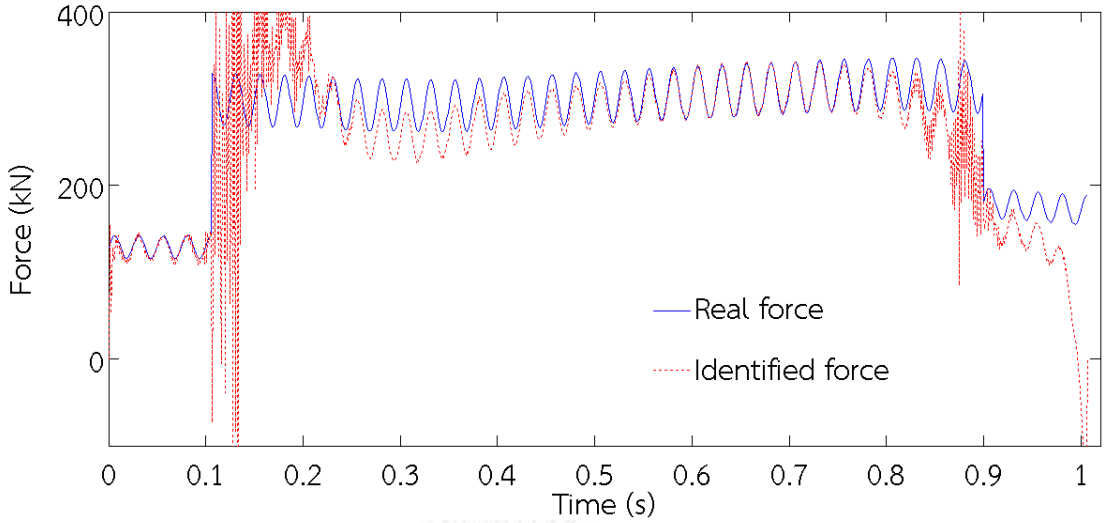

Figure 4.34 Summation of identified forces for v=40m/s

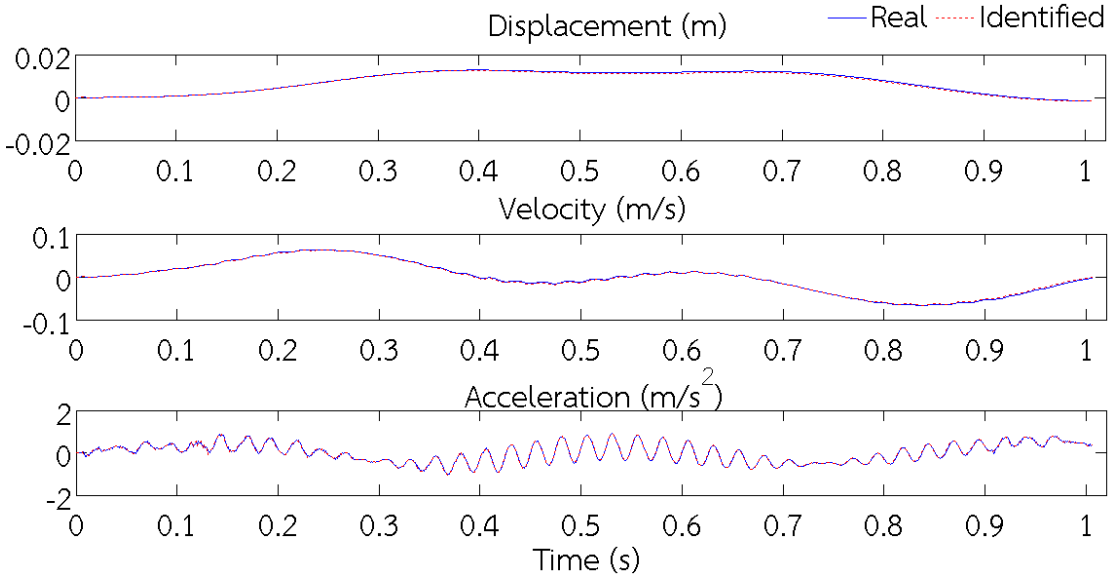

Figure 4.35 Identified responses at mid-span for v=40m/s

From the obtained results, it is obviously seen that the speed of vehicle is an important factor in force identification. It can be observed that for speed v=5m/s the error between real and identified force is significant. In addition, similar error exists on the figure of reproduced displacement, while acceleration and velocity responses are quite accurate. However, for speed=40m/s, these errors cannot be observed neither at the figure of identified force or reproduced displacement.

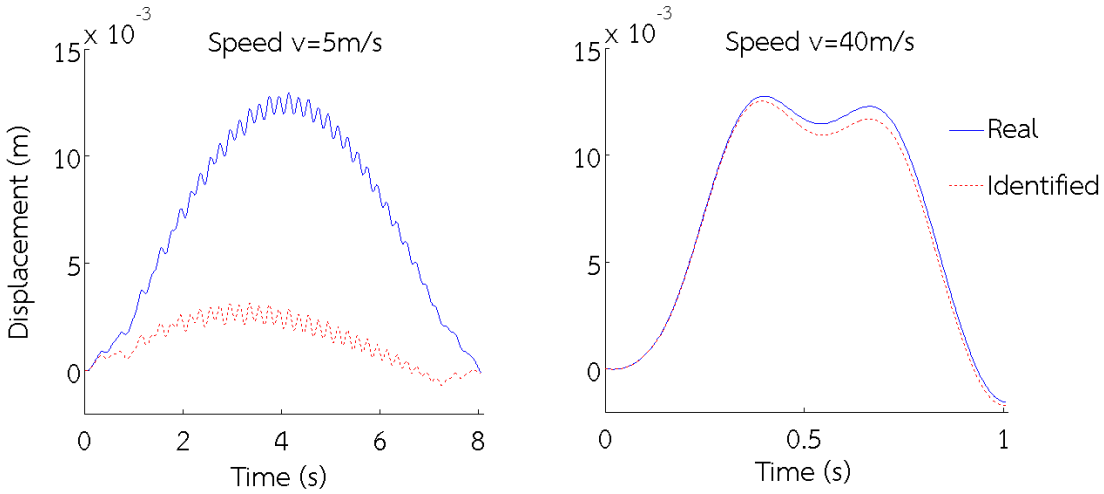

Figure 4.36 Comparison of identified displacement at mid-span for v=5m/s and v=40m/s

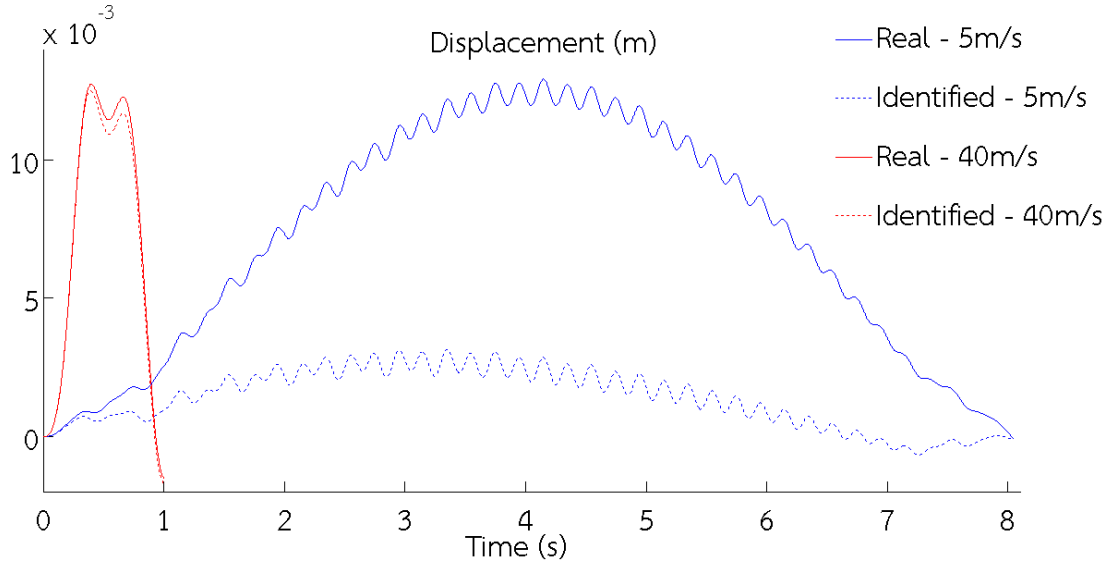

Figure 4.37 Comparison of identified displacement at mid-span for v=5m/s and v=40m/s

It seems that higher speed of vehicle reduces the error between identified and real dynamic force. The reason is that for moving vehicle with high speed, the system has dynamic pattern as shown in Figure 4.37. The similar relation was observed in paragraph 4.5.1.2, which presented that for higher additional force, reproduction of responses was more accurate.

Table 4.12 Identification error for different speeds of vehicle

Speed [m/s]	Error[%]					
	Front	Rear	Sum	$\ddot{x}$	$\dot{x}$	x
5	73.26	92.07	83.82	1.35	35.83	80.89
10	33.47	62.61	45.75	5.29	32.56	37.96
15	33.13	50.26	28.14	5.04	18.31	19.06
20	38.20	49.75	21.37	7.37	11.94	11.47
25	61.61	47.85	25.21	7.83	8.48	7.26
30	47.62	51.62	20.49	7.38	6.03	6.05
35	51.08	51.16	22.97	7.93	4.83	4.90
40	50.99	51.82	22.98	7.56	3.73	4.39

As shown in Table 4.12, the higher speed of vehicle, the more accurate identification of dynamic force is obtained. With the increase of the speed of vehicle, the accuracy of reproduced displacement and velocity increase, although the accuracy of acceleration response decreases significantly.

For higher speeds the most accurate is summation of both axles. This suggests the use of summation of identified dynamic forces to approximate the weight of moving vehicle.

In addition, the influence of time step on accuracy is checked. Since the axle loads identification is the most accurate for vehicle moving with the speed 40m/s, this speed is applied to the vehicle in the numerical example. Four time steps are investigated: dt=0.0002, 0.001, 0.0005 and 0.00025 s.

Table 4.13 Identification error for different time steps

Time step [s]	Error[%]					
	Front	Rear	Sum	⠿	⠭	⠼
0.002	43.33	92.01	51.19	12.76	8.85	10.49
0.001	50.99	51.82	22.98	7.56	3.73	4.39
0.0005	53.69	56.84	24.51	4.99	1.92	3.10
0.00025	41.51	49.17	27.26	3.78	1.24	2.48

The accuracy of force identification and response reproduction increases for smaller time steps. For time step equal to dt=0.001s, the accuracy of obtained results is satisfying, since acceleration error is less than 8%. Further reducing the size of time step seems to be impractical because the improvement in accuracy is not significant, while the computation time increases dramatically. Due to good accuracy for this time step dt=0.001, it is chosen as representative and is used in all simulations of weight estimation.

4.5.2 Weight estimation

This section studies weight estimation of moving vehicle over the bridge deck. The movement of vehicle over the bridge can be divided into three intervals. The 1st interval is from the time zero, when front axle enters the bridge to the time when rear axle enters the bridge. The 2nd interval is the time when two axles of the vehicle are on the bridge deck. The last interval is time when only rear axle is on the bridge deck. To identify weight of front and rear axle, the algorithm is divided into two parts.

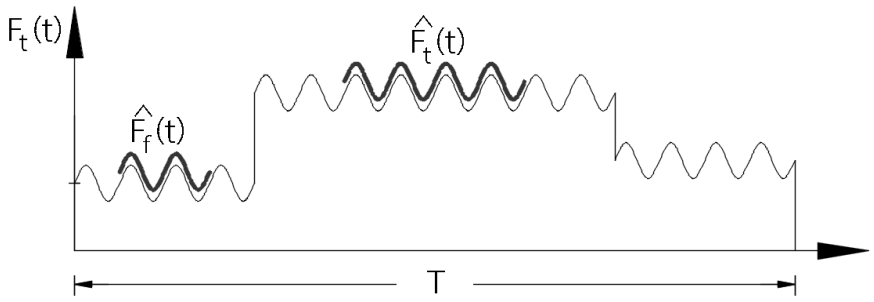

Figure 4.38 Weight estimation scheme

$$\widehat{N_f} = average\ of\ \widehat{F_f}(t) \tag{4.3}$$

$$\widehat{N_t} = average\ of\ \widehat{F_t}(t) \tag{4.4}$$

$$\widehat{N_r} = \widehat{N_t} - \widehat{N_f} \tag{4.5}$$

The first part covers force identification only when front axle is moving over the bridge (1st interval). To identify weight of front axle, central time period equal to 50% of whole interval is used to remove the undesirable influence of support conditions. The weight of front axle is assumed to be the average of identified dynamic force.

In the second part, force identification covers all movement of vehicle over the bridge (three intervals together). Firstly the summation of identified axle forces is done. Then, time period equal to 50% of the 2nd interval (when two axles are on the bridge) is used to identify summation of forces. Finally subtraction between the average of summed identified forces and estimated weight of front axle from the 1st part is made to identify weight of rear axle as shown in Figure 4.38.

The idea of using 50 % of interval gives better accuracy and reduces errors due to enter and exit of front and rear axles on the bridge. Additionally to study accuracy of identified weight, the relative percentage errors are calculated based on average identified force and real weight.

$$error_F = \frac{\left\|\widehat{N_f} - N_f\right\|}{\|F_f\|} \cdot 100\% \tag{4.6}$$

$$error_F = \frac{\left\|\widehat{N_r} - N_r\right\|}{\|F_r\|} \cdot 100\% \tag{4.7}$$

$$error_F = \frac{\left\|\widehat{N_t} - N_t\right\|}{\|F_t\|} \cdot 100\% \tag{4.8}$$

Where $\hat{N}$ and N denote the average identified load and static weight of axle, respectively. The indices f, r and t denote front axle, rear axle and summation of both axles, respectively.

4.5.2.1 Axle spacing

The same properties of the vehicle are considered as in the 4.5.1.1. Three axle spacing are investigated: 0.5S, S and 1.5S, where S= 4.27m to address the accuracy of weight estimation for different width of axle spacing.

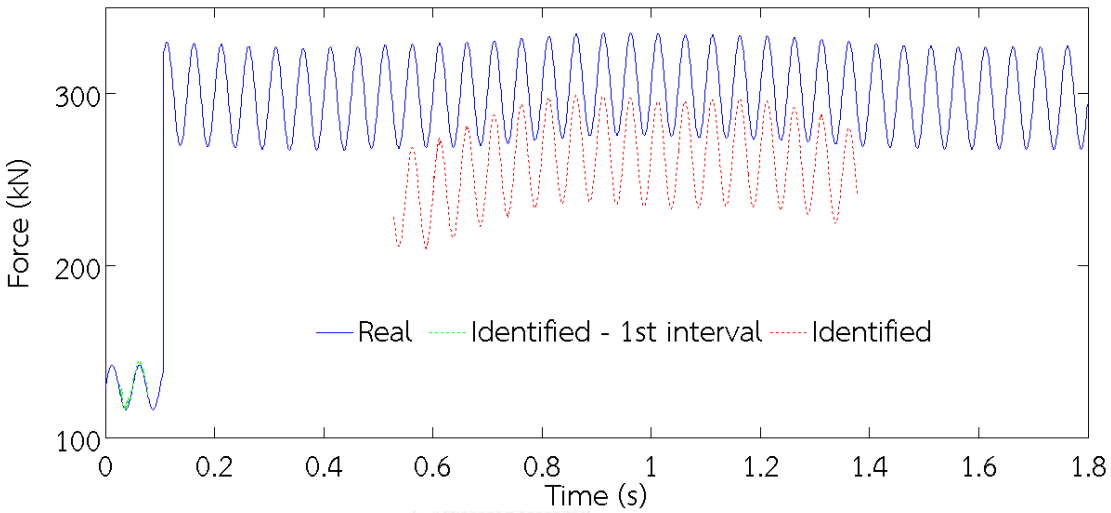

Figure 4.39 Summation of identified forces for 0.5S

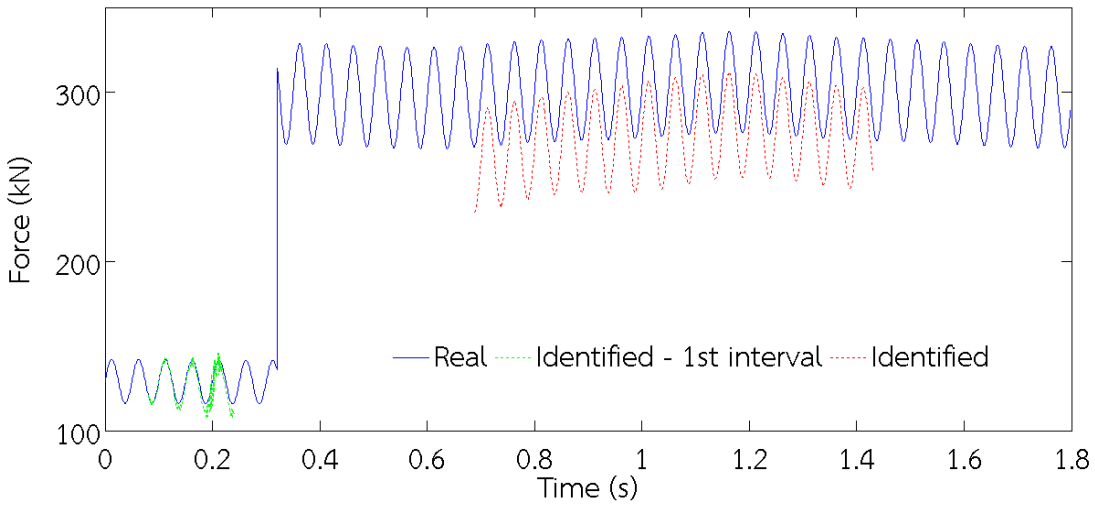

Figure 4.40 Summation of identified forces for 1.5S

Table 4.14 Identification error for different axle spacing

Axle spacing	Error[%]		
	Front	Rear	Sum
0.5S	-1.33	24.73	13.52
S	-0.21	19.09	10.78
1.5S	2.55	13.67	8.88

As shown above, the weight estimation of front axle is quite accurate for all axle spacing, no significant difference in error can be observed. For wider axle spacing, the accuracy of weight estimation of rear axle increases significantly. This indicates that weight estimation is more accurate for wide axle spacing.

4.5.2.2 Mass of vehicle

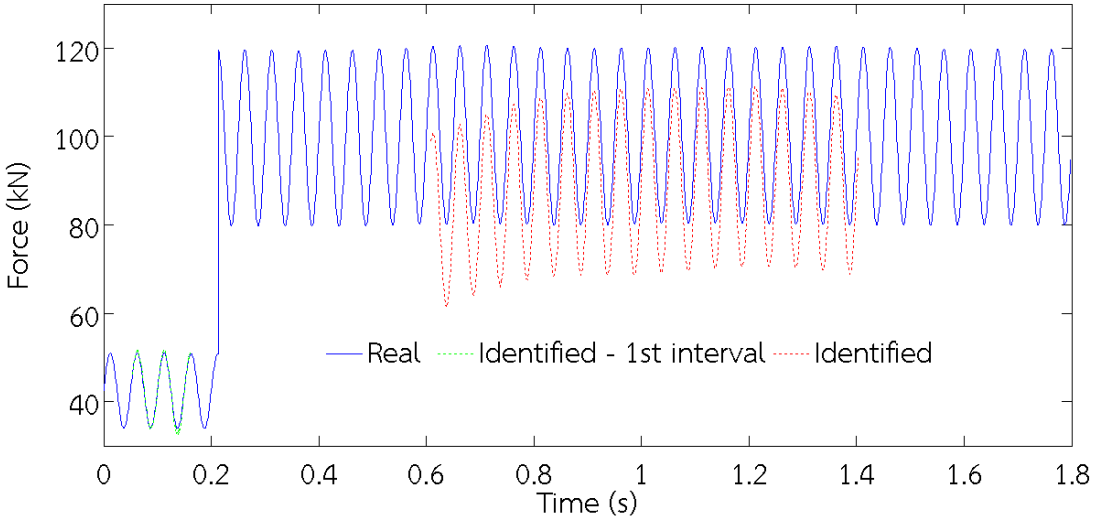

Figure 4.41 Summation of identified forces for N_t=100kN, F_{add}=20%

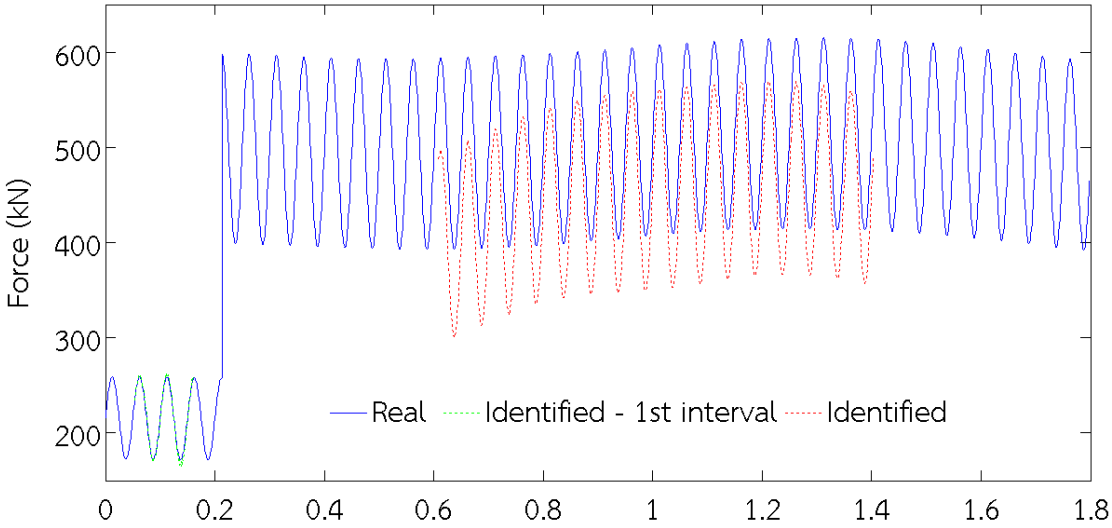

Figure 4.42 Summation of identified forces for N_t=500kN, F_{add}=20%

As shown in the figures above, the accuracy of weight estimation does not depend on the weight of the vehicle or the percentage of additional force applied to the system. The difference between the errors of summed weights between N_t = 100kN and N_t = 500kN is not significant, is around 1%.

Table 4.15 Identification error for N_t = 100kN

Fadd	Error[%]		
	N_t = 100kN		
	Front	Rear	Sum
0	0.42	19.42	11.34
10%	-0.22	19.97	11.39
20%	-0.85	20.52	11.43
Average	-0.22	19.97	11.39

Table 4.16 Identification error for N_t = 200kN

Fadd	Error[%]		
	N_t = 200kN		
	Front	Rear	Sum
0	0.42	19.23	11.15
10%	-0.22	19.78	11.20
20%	-0.85	20.34	11.25
Average	-0.22	19.78	11.20

Table 4.17 Identification error for N_t = 300kN

Fadd	Error[%]		
	N_t = 300kN		
	Front	Rear	Sum
0	0.42	18.53	10.74
10%	-0.21	19.09	10.78
20%	-0.85	19.65	10.83
Average	-0.21	19.09	10.78

Table 4.18 Identification error for N_t = 400kN

Fadd	Error[%]		
	N_t = 400kN		
	Front	Rear	Sum
0	0.42	18.02	10.43
10%	-0.21	18.58	10.48
20%	-0.85	19.13	10.52
Average	-0.21	18.58	10.48

Table 4.19 Identification error for N_t = 500kN

Fadd	Error[%]		
	N_t = 500kN		
	Front	Rear	Sum
0	0.42	17.86	10.34
10%	-0.21	18.42	10.38
20%	-0.85	18.98	10.43
Average	-0.21	18.42	10.38

4.5.2.3 Speed of vehicle

This part will show the relation between the accuracy of identified weights and speed of vehicle. The same properties are considered in this numerical simulation as in 4.5.1.3.

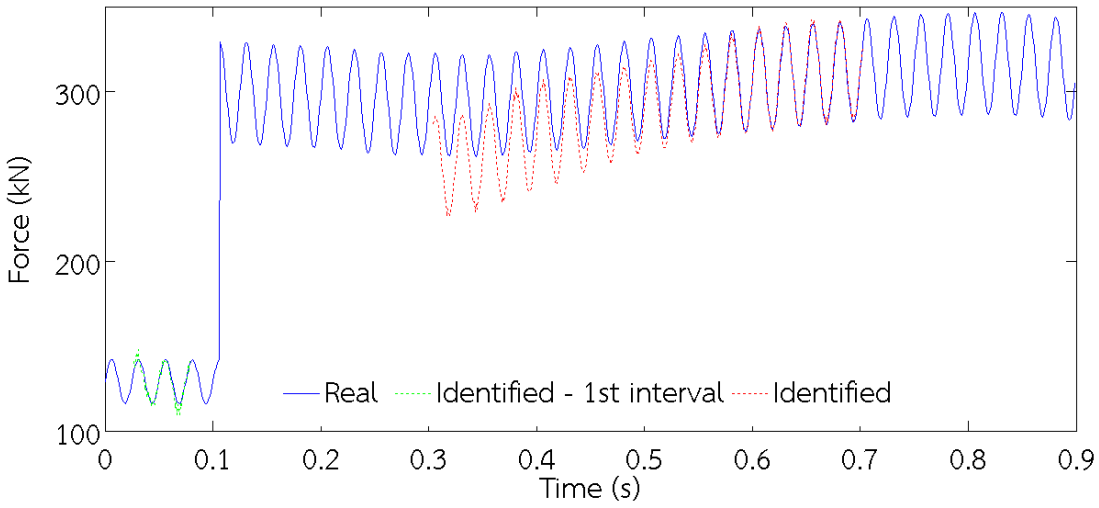

Figure 4.43 Summation of identified forces for v=40m/s

Table 4.20 Identification error for different speeds of vehicle

Speed [m/s]	Error[%]		
	Front	Rear	Sum
5	6.51	136.25	80.41
10	-1.87	66.16	36.88
15	-0.55	33.07	18.60
20	-0.21	19.09	10.78
25	0.26	11.34	6.57
30	0.21	8.68	5.03
35	0.19	7.09	4.12
40	0.36	6.37	3.78

It seems that the speed of vehicle is a main factor which influences the accuracy of weight estimation as it was for dynamic force identification. For speed of vehicle higher than 10m/s, estimated weight of front axle is very accurate; the error is always less than 1%. To estimate weight of rear axle, the speed of vehicle should be higher than 25m/s to obtain error less than 10%. That is why in future application the method should be used only when minimum speed limit is achieved.

In conclusion, the accuracy of weight estimation depends greatly on the axle spacing and speed of vehicle. The relation between these factors and error of identified weight is shown in Figures 4.44, 4.45 and 4.46. It is clearly seen from these figures that weight estimation of front axle is accurate for any axle spacing and speed higher than 5m/s, the error is less than 5%. The estimation of rear axle and summation of axles is the most accurate for high speed and wide axle spacing. It should be noted that speed of vehicle is the significant factor in weight estimation and the influence of axle spacing may not be considered.

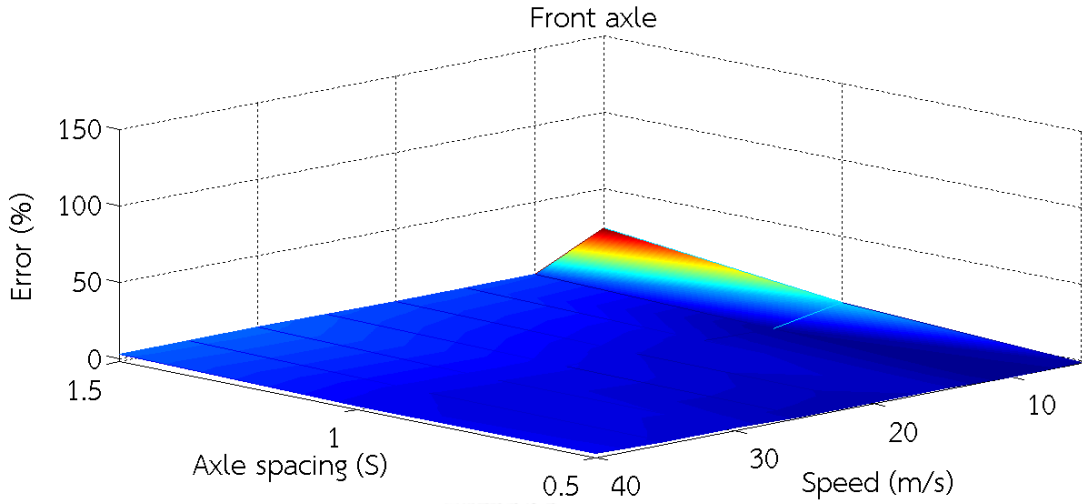

Figure 4.44 Error of front axle for different axle spacing and speed

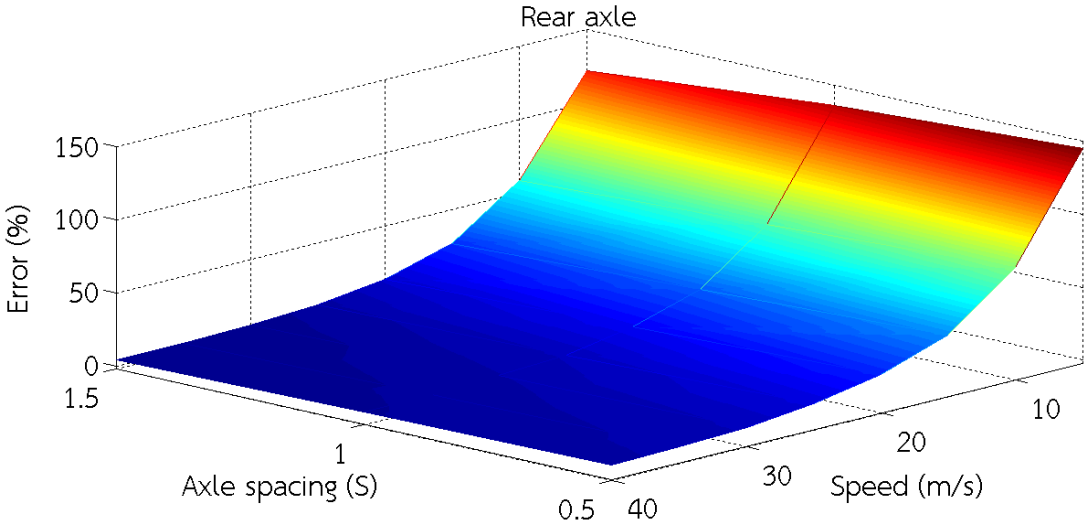

Figure 4.45 Error of rear axle for different axle spacing and speed

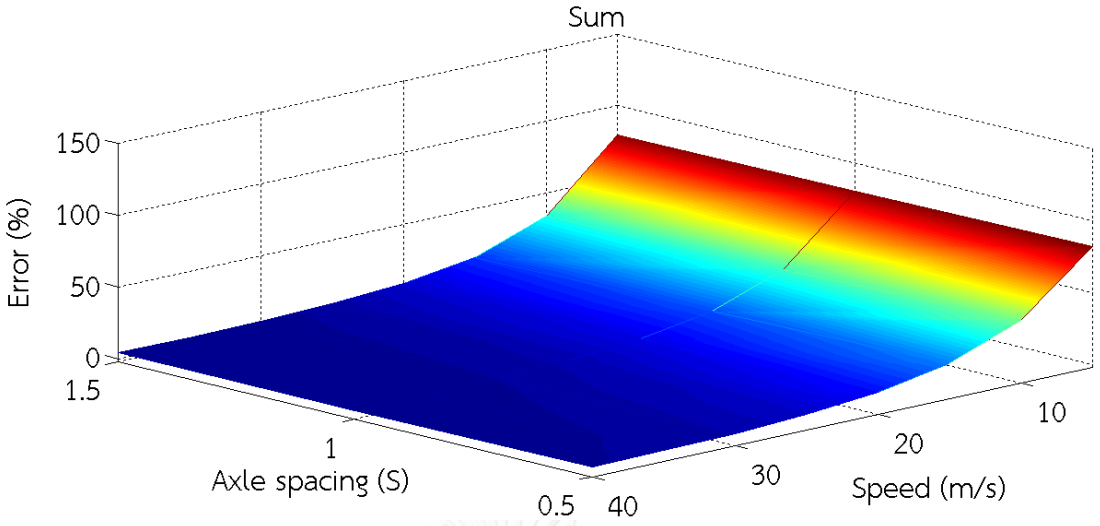

Figure 4.46 Error of summation of axles for different axle spacing and speed

5. Conclusion

The average acceleration discrete algorithm is proposed to identify moving load passing over the bridge. Numerical analyses of four systems are conducted. Vehicle is simplified as a single point load or as 4 degrees of freedom model. Three models of bridge system consisting of SDOF, MODF with non-moving load and MDOF with moving load are investigated.

For SDOF system, force identification is accurate for all considered load functions. The identification errors of less than 10% are expected. It is possible to identify not only continuous force, but also impact force in which its magnitude changes abruptly. Load identification for either constant or sinusoidal load functions reveals similar results. This implies that fluctuation of the load does not significantly affect the accuracy.

For MDOF system with non-moving load, larger errors of the identified loads can be observed. This implies that the accurate load identification demands higher mode information to precisely reproduce the acceleration response of MDOF system.

For MDOF system with moving load, unlike previous cases, the identification errors of the loads are found very large (>100%) although the errors of the acceleration are well within 10%. This is caused by the ill conditioned system when the load position is close to the bridge support. Although the reduction of time step size can enhance the identification accuracy, the required step size seems to be impractical.

For MDOF system with moving vehicle, the impact of different vehicle properties on accuracy has been studied. To reduce the error connected with ill-conditioned system the optimal regularization parameter λ was applied to the system.

For identification of dynamic interaction force and estimation of weight, the same conclusions have been made. Mass of vehicle and the additional force do not change the accuracy of identification. The most important factors are axle spacing and speed of vehicle. The best accuracy was obtained for the widest axle spacing and high speed. That is why, in application this method should be used only when minimum speed limit is guaranteed.

REFERENCES

1. Chan, T.H., S. Law, and T. Yung, *Moving force identification using an existing prestressed concrete bridge.* Engineering Structures, 2000. 22(10): p. 1261-1270.
2. Chan, T.H., et al., *An interpretive method for moving force identification.* Journal of Sound and Vibration, 1999. 219(3): p. 503-524.
3. Chan, T.H., L. Yu, and S. Law, *Comparative studies on moving force identification from bridge strains in laboratory.* Journal of Sound and Vibration, 2000. 235(1): p. 87-104.
4. Chan, T.H. and T. Yung, *A theoretical study of force identification using prestressed concrete bridges.* Engineering Structures, 2000. 22(11): p. 1529-1537.
5. Deesomsuk, T., *Identification of moving vehicle loads from bridge bending moments*, in *Civil Engineering*. 2008, Chulalongkorn University: Bangkok, Thailand.
6. Ding, Y., et al., *Average acceleration discrete algorithm for force identification in state space.* Engineering Structures, 2013. 56: p. 1880-1892.
7. Feng, D., H. Sun, and M.Q. Feng, Simultaneous identification of bridge structural parameters and vehicle loads. Computers & Structures, 2015. 157: p. 76-88.
8. Frýba, L., *Vibration of solids and structures under moving loads*. Vol. 1. 2013: Springer Science & Business Media.
9. Henchi, K., et al., *An efficient algorithm for dynamic analysis of bridges under moving vehicles using a coupled modal and physical components approach.* Journal of Sound and Vibration, 1998. 212(4): p. 663-683.
10. Law, S., et al., *Vehicle axle loads identification using finite element method.* Engineering Structures, 2004. 26(8): p. 1143-1153.
11. Law, S., T.H. Chan, and Q. Zeng, *Moving force identification: a time domain method.* Journal of Sound and vibration, 1997. 201(1): p. 1-22.

12. Lu, Z. and J. Liu, *Identification of both structural damages in bridge deck and vehicular parameters using measured dynamic responses.* Computers & Structures, 2011. 89(13): p. 1397-1405.

13. Pinkaew, T., Identification of vehicle axle loads from bridge responses using updated static component technique. Engineering Structures, 2006. 28(11): p. 1599-1608.

14. Qiao, B., et al., *A force identification method using cubic B-spline scaling functions.* Journal of Sound and Vibration, 2015. 337: p. 28-44.

15. VII, E.C.D., Transport: Weight-in-motion of Axles and Vehicles for Europe (WAVE). 2001.

16. Wang, T., et al., *A novel state space method for force identification based on the Galerkin weak formulation.* Computers & Structures, 2015. 157: p. 132-141.

17. Wu, S. and S. Law, *Moving force identification based on stochastic finite element model.* Engineering Structures, 2010. 32(4): p. 1016-1027.

18. Xu, X. and J. Ou, *Force identification of dynamic systems using virtual work principle.* Journal of Sound and Vibration, 2015. 337: p. 71-94.

19. Xu, Y., et al., *Stress and acceleration analysis of coupled vehicle and long-span bridge systems using the mode superposition method.* Engineering Structures, 2010. 32(5): p. 1356-1368.

20. Yang, Y. and C. Lin, *Vehicle–bridge interaction dynamics and potential applications.* Journal of sound and vibration, 2005. 284(1): p. 205-226.

21. Yu, L. and T.H. Chan, *Moving force identification based on the frequency–time domain method.* Journal of Sound and Vibration, 2003. 261(2): p. 329-349.

22. Zhu, X. and S. Law, *Identification of moving interaction forces with incomplete velocity information.* Mechanical Systems and Signal Processing, 2003. 17(6): p. 1349-1366.

23. Zhu, X. and S. Law, *Moving load identification on multi-span continuous bridges with elastic bearings.* Mechanical Systems and Signal Processing, 2006. 20(7): p. 1759-1782.

VITA